2019

Remote Sensing of Avalanche Paths in Glacier National Park, Montana

Morgan Voss
University of Montana

REMOTE SENSING OF AVALANCHE PATHS

IN GLACIER NATIONAL PARK, MONTANA

By

MORGAN ANN ELIZABETH VOSS

B.S. Geology, University of Oregon, Eugene, OR, 2013
B.S. Geography, University of Oregon, Eugene, OR, 2013

Thesis

presented in partial fulfillment of the requirements
for the degree of

Master of Science
in Geography

The University of Montana
Missoula, MT

December 2018

Approved by:

Scott Whittenburg, Dean of the Graduate School

Dr. Anna Klene, Chair
Department of Geography

Mr. Erich Peitzsch,
Department of Geography

Dr. Lloyd Queen
Department of Forest Management

Voss, Morgan, A.E. M.S., Fall 2018 Geography

Remote sensing of avalanche paths in Glacier National Park, Montana

Committee Chair: Dr. Anna Klene

Snow avalanches are the common form of mass wasting in the high mountain environments of Glacier National Park (GNP), Montana. These natural disturbances play important roles in mountain ecosystems by regularly disturbing montane systems, providing critical habitat for some species, transporting debris, and influencing vegetation and fire dynamics. Since the 1900s, natural avalanche-related activity recorded along important transportation corridors within the park has frequently disrupted transportation.

While many of the steep slopes of GNP are susceptible to avalanching, formal inventories exist only for small, critical portions of the park and they vary substantially from one another. GNP's protected status does not allow for avalanche mitigation, allowing this area to serve as a natural mountain environment for studying these processes. A current, high-resolution inventory of avalanche locations in the park is needed for the entirety of the Park.

Imagery and digital elevation models (DEMs) were used to map the distinct biogeographic and topographic patterns left by avalanching using machine learning methods. Mosaics of National Agricultural Imagery Program (NAIP) aerial photographs acquired in 2013 were segmented to map avalanche tracks. Principal components from the imagery and derivatives of the DEM were used as input to a Random Forests algorithm which mapped the most likely class for each segment using a probabilistic approach. Avalanche paths were found to comprise approximately 5-12% of the park, along predominantly south and southeasterly facing slopes between 20° to 40°. While this estimate is similar to previous studies, this work did not map starting or runout zones which would have increased the total area. The paths predicted provide a comprehensive inventory that can be used to monitor shifts in vegetation and climate dynamics within the disturbance regime. Changes were clearly seen in the contraction and expansion of trim lines of some avalanche paths in recent imagery. Future research could use this work as a baseline for time-series analysis.

TABLE OF CONTENTS

ACKNOWLEDGEMENTS

I am eternally grateful for the many mentors, colleagues, and friends who supported me throughout my graduate school career. First, I would like to thank my advisor, Dr. Anna Klene, who consistently dedicated her time and insight to this project, as it was a particularly interesting one from the very beginning. I am thankful for benefitting from her experience in remote sensing and grateful for the knowledge she provided throughout this research. I would also like to thank my committee members, Dr. Lloyd Queen and Mr. Erich Petizsch, who both offered valuable information throughout the course of the project.

In particular, this project would not have been possible without the support of the USGS in West Glacier. Dr. Dan Fagre and Erich Peitzsch were especially significant in crafting the development of this project throughout its many changes. Their knowledge of avalanching and mountain ecosystems is unsurpassable and was extremely valuable throughout this entire process. I am extremely grateful for them giving me the opportunity to perform research in Glacier National Park; the amount I have learned from them alone is substantial and has made me a better scientist overall. I am also very grateful for the ideas from Rebecca Kranitz, who initially started this project, and graciously passed it on to me while she pursued other academic interests.

This project would not have been possible without USGS funding, but also support from the Montana Association of Geographic Information Professionals (MAGIP), Red Castle Resources, NPS staff, and the Glacier National Park Conservancy. I am very thankful for the Jerry O'Neal Fellowship from the GNP Conservancy which allowed me to finish research and gain more field experience over the summer. In addition, the help from Dr. Rob Ahl and John Hogland was crucial to this project; thanks for your insight and answering of my countless questions.

Lastly, I'd like to thank my partner, Sam, for his undaunted support and flexibility with my insane, highly committed graduate school schedule. Thanks for your positivity, encouragement, and reality checks.

LIST OF FIGURES

LIST OF TABLES

APPENDIX TABLES

1 INTRODUCTION

Avalanche disturbances are vital events in the natural dynamics of mountain ecosystems, especially the mountain ecosystems of Glacier National Park (GNP) in northwestern Montana (Fig 1). Even casually observing the landscape of GNP reveals the prevalence of avalanche paths. Within the park, avalanches play an important role in disturbance ecology, serving as important habitat for many key ecosystem species, such as the grizzly bear and wolverine. In addition to their importance in wildlife habitat, avalanches affect forest composition, carbon sequestration, and nutrient flows. The amount of influence avalanches exert in this alpine ecosystem has been increasingly appreciated by land managers. Monitoring avalanche frequency and magnitude contributes to many land management directives, informs park officials, transportation planners, recreationists, and others.

Figure 1. Glacier National Park is located in northwestern Montana.

Avalanches are a mass wasting process, in which the frequency and magnitude of large-scale events is controlled by snowpack, weather, and climate factors (Fagre & Peitzsch, 2010). Declining snowpack is well documented through historic meteorological records, however, the impact of changing snowpack characteristics on avalanche frequency and magnitude is inconclusive in high alpine environments, likely due to the growth of explosive mitigation techniques in avalanche control (Schneebeli et al., 1997; Bellaire et al., 2016). However, since GNP's protected status does not allow for induced avalanche control measures, analyzing recent landscape dynamics allows for further understanding of the geomorphic, ecological, and societal impacts of avalanches in the GNP mountain environment in context of a changing climate.

Extreme weather events that trigger large magnitude avalanches may become more common with changing climate, affecting locations and frequency of the events (Fagre & Peitzsch, 2010). In particular, changes in magnitude or frequency impact geomorphology by amounts of debris flow, land-cover in terms of forest and shrub cover, and forest characteristics including the locations, destruction, or regrowth of mature forest stands. These distinct swaths left by avalanche events are often described as "natural fire breaks" (Malanson & Butler, 1984) and can influence fuel distribution. The effects on mature forest stands from avalanche events can substantially change forest stand dynamics and composition, a factor for land managers to consider concerning transportation infrastructure, fire ecology, and land cover management.

Snow avalanche disturbance regimes have left distinct imprints on mountain landscapes within GNP. Since the 1900s, natural avalanche-related activity has created numerous incidents involving transportation infrastructure on the southern border of GNP,

in addition to biogeomorphic impacts. Many known snow avalanche paths exist on the Going-to-the-Sun Road (GTSR), and John F. Stevens (JFS) Canyon, along U.S. Highway 2 on the southern border of the park (Fig. 2). JFS Canyon, which separates GNP from the Bob Marshall Wilderness complex to the south, is home to the highway and railway and numerous wildlife corridors. The locations and characteristics of avalanche paths in these areas have been the focus of most previous studies.

Understanding the characteristics of these avalanche events (such as size and spatial distribution) is crucial for assessing disturbance regimes and their link to social-ecological systems. A complete dataset documenting the locations and frequencies of events in snow avalanche paths in GNP would be extremely useful for monitoring for change through time. While several studies document locations of avalanche paths throughout the park (Butler, 1979; Butler, 1990; Carrera, 1990; Hamre & Overcast, 2004; USGS, 2007; Steiner et al., 2012; Peitzsch & Fagre, n.d.), a park-wide inventory has not been completed.

Perhaps the closest to an inventory comes from a land-cover classification (1999, updated in 2007) which contained an "avalanche-burial" class, described as shrublands identified in an avalanche/snow burial zone, or shrublands where the density of plant growth decreases as elevation increases including vegetation associated with a gradational or transitional pattern (USGS, 2007). This dataset was a decade old when this current effort began, did not have an accompanying accuracy assessment of this category, and did not reflect recent changes in avalanche ecology, or any other disturbances in the park. Because of potential changes in avalanche ecology, magnitude, and frequency, creating a park-wide easily replicable inventory of avalanche tracks in GNP in order to establish baseline measurements for future studies is important.

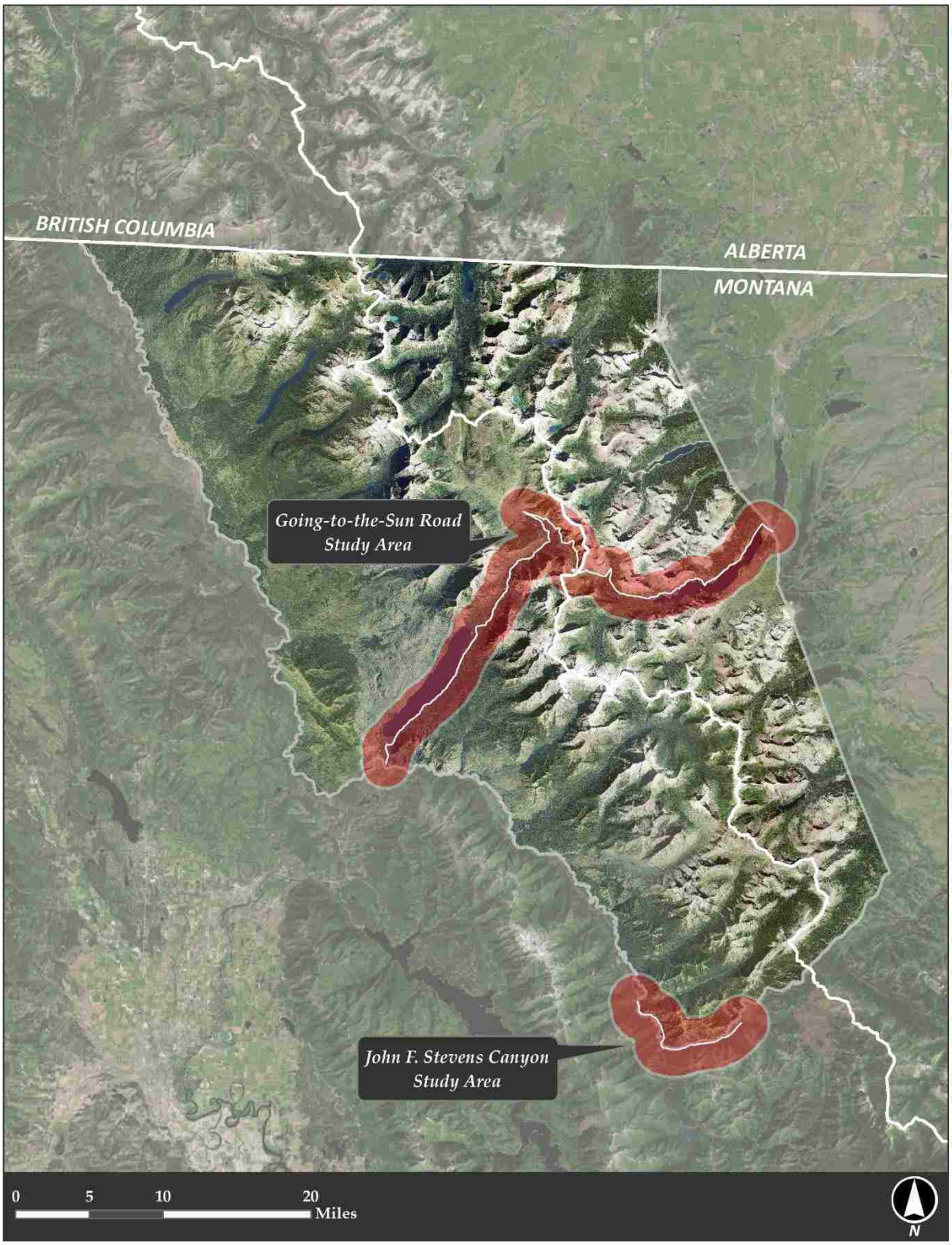

Figure 2. The two most studied avalanche areas in GNP (represented as area within grey polygon) are along the two transportation routes crossing the park (Going-to-the-Sun Road and US Highway 2), which present the most risk to GNP personnel and the public. Continental Divide is shown as a white line.

2 STUDY AREA

GNP, in northwest Montana's Rocky Mountains, is over 4000 km^2 (1 million acres), and made up of steep, rugged terrain with substantial relief above and below treeline. The landforms were carved from Pleistocene and Holocene glaciations. Glacial valleys in the park align northeast to southwest, with slopes in the valley bottoms typically around 30° to 40° (Butler, 1986). The steep slopes within GNP are prime avalanche terrain, and tend to follow a directional control aligned with Pleistocene glaciated valleys (Butler, 1979).

The continental divide passing through the park creates two distinct climate zones – one with Pacific maritime influence to the west, and one with Arctic continental influence to the east (Finklin, 1986). The west has moderate temperatures and more precipitation, the east has windier, drier, and extreme temperature conditions. Precipitation across the park is particularly variable at higher elevations. The GTSR crosses the Continental Divide at Logan Pass at 2,026 m (6,646 ft) and JFS Canyon is just west of the Continental Divide and Marias Pass at 1,589 m (5,213 ft). Both regions are exceptionally avalanche prone areas with steep topography (Martinka, 1972).

3 BACKGROUND

Avalanches are destructive, natural events which dramatically impact landscapes. Early avalanche research took place largely in Europe, although recently more countries have expanded their research into avalanche dynamics (Ancey, 2016).

3.1 Geomorphology and Ecology of Avalanches

During the 1960s, North American researchers became very attentive to hazard assessments due to the advancement of transportation framework across the west (Luckman, 1978). These hazard-targeted studies largely focused on avalanche causes, hazard, magnitude, and frequency, but seldom on the underlying geomorphic or ecologic processes. However, Rapp (1960) proposed that "dirty" avalanches capable of impacting landscapes by carrying plant and rock material with debris flows, while "clean" avalanches did not affect the landscape. Luckman (1977) identified topographic conditions, snow, vegetation cover, and debris availability as factors controlling the geomorphic impacts of snow avalanches. He tested the influence of these factors in the Canadian Rockies (1978) and concluded that the geomorphic effects and depositional landforms resulting from avalanche activity demonstrated their role in debris transfer. Using tree-ring dendrochronology and avalanche-scarred trees in the Canadian Rockies, Johnson (1987) found a correlation between density and heights of vegetation and trees in avalanche paths and the frequency of persistent avalanches. Patten and Knight (1994) found similar results in Cascade Canyon, Grand Teton National Park, Wyoming.

Using tree-ring analysis to discover the frequencies of avalanche events has become a standard practice, especially in areas with few historical avalanche records (Pederson et al., 2006; Schläppy et al., 2013; Ballesteros-Cánovas et al., 2018). Studies in GNP have sought to characterize frequency largely near the southern park boundary (e.g. Butler & Malanson, 1985; Pederson et al., 2006; Butler et al., 2010).

3.2 Remote Sensing of Avalanche Paths

Applied GIS technologies allow researchers to study both larger and more remote areas using aerial photos, satellite imagery, and/or digital elevation models (DEMs) from imagery or LiDAR. The increasing availability of remotely sensed imagery (particularly low-cost) has made it possible to study spatial patterns over larger areas and change through time, allowing for landscape-scale analyses (Turner et al., 2001).

Considered a key ecosystem disturbance (Walsh et al., 2004; Turner, 2010), avalanches often carry debris and/or erode the landscape. These "scars" are noticeable and well suited for studying the spatial arrangement and influences involved in the spread of disturbance processes (Gökyer, 2013). Avalanche tracks typically consist of elongated patches of shrub and forb regrowth, clearly noticeable on the ground and in imagery of ~30 m resolution or finer.

The green, elongated patches (a mix of shrubs and deciduous trees) are far from the most common vegetation cover within GNP (USGS, 2007), but are obvious when viewed in both satellite and oblique imagery. However, the spectral signatures of shrubs and forbs in avalanche tracks are to those same species found in low elevations and near river channels. Previous avalanche track maps in GNP have been field based, focusing on dendrochronology, hazards, or snow science principles (e.g. Peitzsch et al., 2015; Fagre & Peitzsch, 2010; Butler & Sawyer, 2008; Reardon et al., 2008; Pederson et al., 2006; Hamre & Overcast, 2004; Butler & Walsh, 1990).

Advances in remote sensing classification methods have shifted towards machine learning, offering algorithms well suited for complex population distributions. One of these machine learning algorithms (MLAs), the random forest classifier, is an ensemble classifier utilizing multiple decision trees with a subset of training data and predictor

variables (Breiman, 2001). Despite limited availability in remote-sensing software, decision tree and random forests methods are becoming more common within remote sensing literature (e.g. Pal & Mather, 2003; Guan et al., 2012; Belgiu & Drăgut, 2016; Kulkarni & Lowe, 2016). The increased usage of machine-learning algorithms is attributed to the capabilities of the algorithms to model complex class signatures, accept and evaluate many predictor variables, return higher accuracies, estimate individual variable importance, and the ability to accept data of different distributions (e.g. non-parametric vs. parametric; Kulkarni & Lowe, 2016; Maxwell et al., 2018).

MLAs, paired with other techniques, such as image segmentation (which partitions pixels into groups or objects based on similar characteristics), and land-cover classifications are increasingly able to focus on spectrally significant, complicated patterns with object-oriented analysis. The distinct patches and shape dynamics of avalanche tracks are well suited for segmentation and MLAs.

3.3 Avalanche Studies in Glacier National Park

Although studies of avalanche activities within GNP increased in the 1980s and 1990s, research gaps remain. Using ground-based photographs and topographic maps, Butler and Walsh (1990) investigated the lithologic, structural, and topographic constraints on the avalanche paths in eastern GNP, concluding that more than 50% of these paths started under an erosion resistant diorite sill typically at the contact with the softer, underlying Helena limestone. These paths exhibited patterns in slopes and aspect, with many on slopes between 25° and 35°, aligning with many Pleistocene glaciated valleys in a concentration of south, southeast, and northwest facing aspects, (Butler, 1979).

In addition to geologic influences, by looking at the Normalized Difference Vegetation Index (NDVI) and Tasseled Cap transformation vegetation indices, Walsh et al. (2004) found snow avalanches alter the vegetation structures and contribute to post disturbance regeneration in the paths, suggesting different vegetation patterns occur in avalanche paths compared to adjacent forests. Butler (1979) also identified patterns in the distribution of vegetation within these paths, describing the main tree types (*Abies lasiocarpa, Alnus spp.*, and *Acer glabrum*), and finding the number of conifers in relation to deciduous trees decreases upslope as ground cover vegetation is related to moisture conditions in the lithology.

The Continental Divide influences many of the climate and weather controls on avalanches, especially in GNP. Schweizer et al. (2003) advocated two main constraints on snow avalanche events: fresh snow accumulation and air temperature increase (causing related freeze-thaw cycles). Butler (1986) reported these meteorological controls as triggering of avalanche events in GNP. Microclimatic conditions contribute to the type of avalanching present on either side of the divide, but regional circulation patterns can result in winters with synchronous, wide-spread avalanches (Butler, 1986; Reardon et al., 2008). Butler et al. (1986) concluded that years of anomalously high snow pack levels combined with Arctic air intrusions and advection of moist Pacific air created heavy snowfalls, rain-on-snow patterns, and large magnitude avalanche events through dendrochronological analysis of trees within avalanche paths.

Butler and Malanson (1985) performed a dendrochronological study of 48 trees to determine a historic index of high magnitude avalanche events, finding high magnitude events in this region were not isolated, and frequently occurred in temporal and geographic

clusters. Butler (1986) used a historic chronology of major avalanche winters to establish hazard zones, largely along U.S. Highway 2, which were more extensive and more frequent than initially perceived by National Park Service employees. Although limited in their sample size, using the sites of two avalanche paths along U.S. Highway 2.

Butler (1979) had performed initial studies of terrain and vegetation within the snow avalanche paths in the southern and eastern portions of the park. After multiple destructive avalanche events within and adjacent to the park, an avalanche hazard and forecasting program began in 2004 for the transportation corridor in JFS Canyon (Reardon et al., 2004). This avalanche program along U.S. Highway 2 used avalanche cycles from the previous 28 winters, snow telemetry (SNOTEL) data, field observations, and weather data to derive a history of events for forecasting and hazard mitigation purposes (Reardon et al., 2004). They found that avalanches large enough to disrupt highway and railway operations occur predominantly after rain-on-snow events, during periods of dramatic warming, when temperatures clustered near freezing, or when snowfall buried a near-surface faceted layer. This study was crucial in the development of avalanche mitigation programs for the Burlington Northern Santa Fe (BNSF) Railway.

Hamre and Overcast (2004) created an avalanche path atlas for the JFS Canyon area (including attributes such as starting zone elevation, slope angle, runout length, etc.) for the BNSF Railway as part of the 2004 environmental impact statement for avalanche hazard mitigation in GNP. Steiner et al. (2012) created an avalanche path inventory along U.S. Highway 2 and would later utilize this atlas for their risk-assessment interactive web GIS tool in the JFS Canyon area. An atlas focusing on similar characteristics was produced by Peitzsch and Fagre (n.d.) for hazard mitigations involving snow removal operations

along the GTSR in the park during the spring. The design of the atlas focused on illustrating the spatial distribution of paths and providing a baseline for avalanche research and analysis in the park.

4 METHODOLOGY

Avalanche paths (Fig. 3) typically consist of three zones with very heterogeneous composition, (e.g. rock to shrub to woody debris): the starting zone, track, and runout zone. This study focuses on mapping the area in the track of avalanche paths.

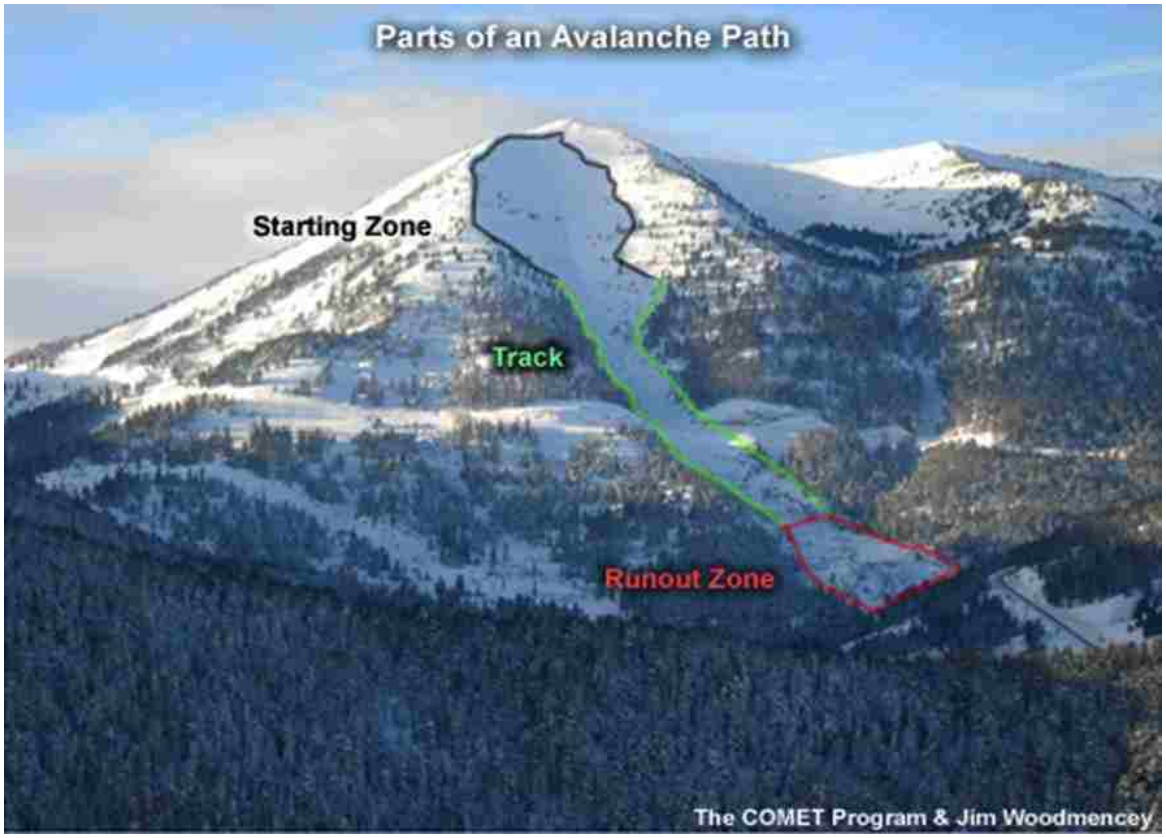

Figure 3. Components of an avalanche path (image courtesy of the University Corporation for Atmospheric (UCAR) at *https://www.meted.ucar.edu/afwa/avalanche/media/graphics/avPaths_partsLabeled.jpg*

4.1 Data Processing

Imagery from the 2013 National Agricultural Imagery Program (NAIP) orthorectified, 1-meter 4-band (R, G, B, NIR) was mosaicked, and clipped to the GNP boundary using Google Earth Engine, a cloud-based remote-sensing platform (Gorelick et al., 2017). The 2013 NAIP imagery acquisition dates for GNP range from early June to early September. Although NAIP imagery is typically collected every two years and made publically available, 2015 was an especially intense wildfire year in Montana prohibiting NAIP data collection over much of GNP. Much of the imagery from 2017 contains snow at higher elevations because the imagery was collected in late October. While higher resolution imagery exists (e.g., WorldView and Digital Globe), NAIP 1-meter imagery was chosen due to the combination of relatively high resolution and open source availability. NAIP imagery mosaics were resampled to match the resolution of the USGS National Elevation Dataset (NED) DEM (10 m).

The landscapes of GNP consist of steep topography and substantial alpine terrain. In order to reduce shadowing, dimensionality, and correlation between bands while retaining information (Lillesand et al., 2014), a principal components analysis (PCA; Fig. 4) was performed in ERDAS Imagine software (Hexagon Geospatial, 2018) on the NAIP mosaic of the park. A majority of the variance was explained in PC1 (92%) while PC2 and PC3 accounted for the other 8% (Table 1).

Principal Component	Eigen Value	Percent of Variance
1	12995.5	92.47
2	956.54	6.81
3	102.14	0.72

Table 1. Principal Components of 4-band 10-m NAIP imagery from 2013.

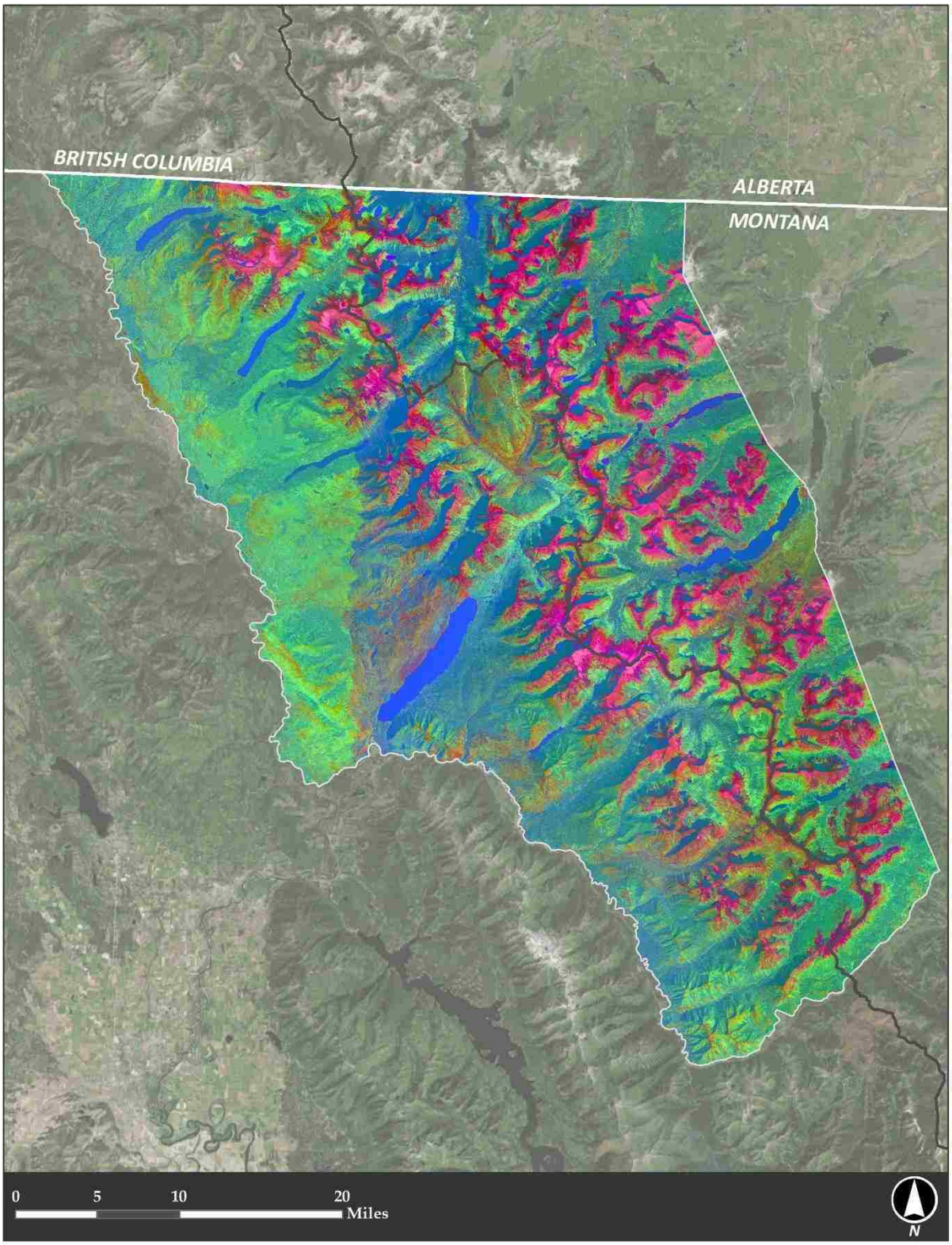

Figure 4. Map of the principal component bands 1, 2, and 3 from resulting from PCA on the 4-band 2013 NAIP imagery after it was coarsened to 10 m. It is a composite RGB image where R is PC1, G is PC2, and B is PC3. Continental Divide is shown as dark gray line.

Using algorithms available in eCognition software (Trimble Geospatial, 2018), segmentation was performed on the first three PCs of resampled 4-band NAIP imagery to extract patches representing avalanche tracks in addition to other land-cover classes. Segments were delineated using multiresolution segmentation, which bases segments on homogeneity definitions in combination with local and global optimization techniques (Baatz & Schäpe, 2010). Segmentation inputs included shape compactness parameters (meaning the closeness or spread of pixels clustered in an object), spectrally similar nearby pixels, and a minimum segment size of 5 pixels. These were exported as vectors in shapefile format, and brought into ArcGIS software (ESRI, 2018) for creation of training and validation data. Shape metrics including a length to width ratio and dispersion (both mean and standard deviation of distances from the segment's centroid) were calculated for each segments.

The elevation data from the NED was mosaicked and clipped to match the NAIP. The DEM was used for elevation and also to calculate derivatives (Table 2) recommended by Maggioni and Gruber (2003).

DEM Raster/Derivative	Purpose
Elevation	Topography
Aspect	Map slopes with more or less solar insolation
Beers Aspect	Aspect transformed into a continuous variable
Slope	Quantifies slope angle
Planar Curvature	Quantifies amount of convexity or concavity

Table 2. Derivatives created from the NED 10-m elevation model used as potential variables in random forest. Beers aspect is a transformation of aspect (when aspect is 0° to 360°) into a continuous variable that ranges from 0-2 with 0 = SW, 1 = NW & SE, and 2 = NE aspects as: Beers aspect = 1 + Cos(45° – aspect) (Beers et al., 1966).

4.2 Random Forest in the Rocky Mountain Research Station (RMRS) Toolbar

4.2.1 Training Data

While random forests and other MLAs offer statistically robust methods aptly suited to handle data of high dimensionality, possible correlation, and complex signatures (Maxwell et al., 2018), each class must be represented in the training data for accurate predictions. Segments were initially selected randomly for training sites for 10 land-cover classes (Table 3). To account for widely differing class frequency, Congalton and Green (2008) recommend a minimum sample size of 50 per class, and an equalized stratified sampling design was used to add samples. The author utilized GNP's prior land-cover classification, photo interpretation, and field visits to increase the total number of training sites for each category to 100 segments between random and user-selected segments.

Class	ID	Random	User Selected
Avalanche Track	1000	9	91
Barren Rock	2000	70	30
Coniferous Forest (Older)	3000	90	10
Fire Scar/Burn	3500	56	44
Shadow	4000	36	64
Shrub/Meadow/Deciduous	5000	41	59
Snow/Glacier	6000	3	97
Water	7000	22	78
Dry Herb/Grassland	8000	36	84
Young Forest/Regeneration	10000	26	74

Table 3. Land-cover classes and the number of training segments selected randomly and those added to reach the minimum number recommended.

4.2.2 Variable Selection

Variables initially considered for prediction and those used in the final random forest classification are in Table 4. The Rocky Mountain Research Station (RMRS) Raster Utility, an ArcGIS add-on software (Hogland & Anderson, 2017) processed the random forest algorithm. The RMRS Raster Utility is an object-oriented coding library that allows

for spatial and statistical analysis using function modeling. Function modeling is raster processing methodology used to create and store transformations of raster datasets that substantially reduces memory usage, processing time, and storage of intermediate steps in large datasets (Hogland & Anderson, 2017). The RMRS Raster Utility's random forest algorithm used zonal statistics to sample the standard deviation and mean values of the variables (Table 4) of the training segments to build a series of decision trees. 34% of the original training data was withheld ("out-of-bag") from the construction of each tree and used for model performance statistics and cross-validation. The remaining data (66%) was utilized to build 500 decision trees. Using the resulting random forest, the RMRS Raster Utility toolbar predicted the most likely class in the defined land-cover categories (Table 3) for all the remaining non-training segments in GNP.

The random forest algorithm generated statistics describing the relative importance of each variable using out-of-bag estimates of classification errors from the withheld training data. All variables were initially modeled and then excluded by relative classification error values (Fig. 5). Final selection of which variables to use to construct the park-wide prediction was based upon assessing how much the relative classification error increased when a variable was excluded from the model. Only one form of each variable was retained, for instance the mean of elevation was statistically more important the standard deviation of elevation, so the mean of elevation was ultimately retained and standard deviation excluded. After removing variables which were below the saturated relative classification error value, a 10.9% relative classification error was achieved.

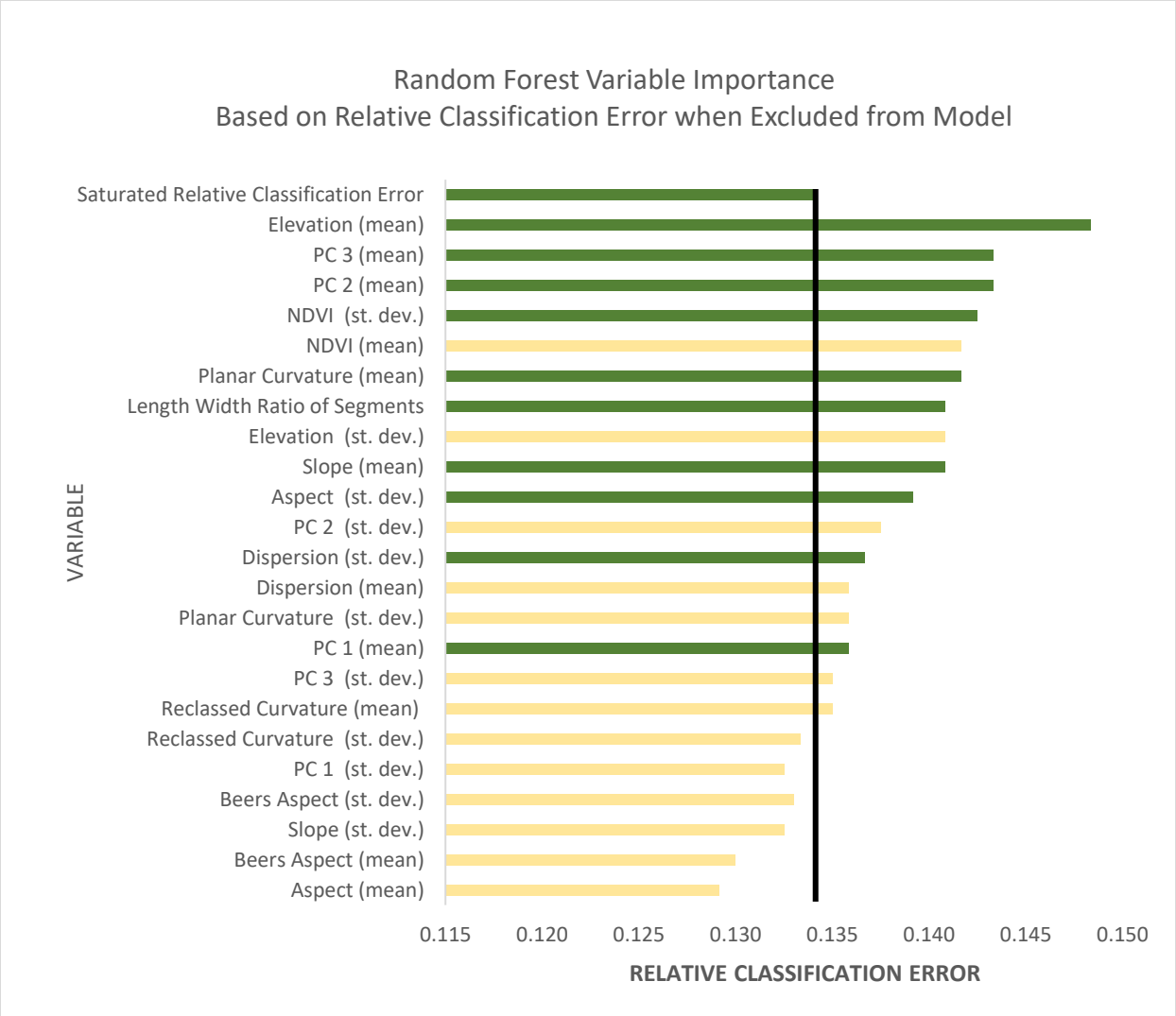

Figure 5. Variable importance in random forest modeling. Variables above the saturated value for relative classification error were included in final modeling. Only the highest of either standard deviation or mean was retained for similar variables. Green bars indicate modeled variables; yellow bars indicate excluded variables.

Category	**Variable**
Imagery	**PC1, PC2, PC3, NDVI***
Terrain	**Elevation, slope, aspect, planar curvature**, re-classed planar curvature (highlighting convex slopes), Beers aspect
Shape Metrics	**Length/width ratio, dispersion (standard deviation of distances from centroids)**, dispersion (mean deviation of distances from centroids)

Table 4. List of variables initially used for prediction in random forest modeling. Those in bold contributed the most to avalanche track relative classification accuracy.
*NDVI is a vegetation index that uses near infrared and red wavelength bands. NDVI = (NIR – Red) / (NIR + Red).

The segments were classified using thresholds based on the number of times out of 500 iterations that a decision tree predicted the segment to be an avalanche track (e.g. 10%, 20%, 30%, 40%, or 50%). In other words, several layers generated with segments with the most likely category of avalanche track above each of several thresholds (segments where p_1000 > 0.3, 0.4, and 0.5).

4.3 Accuracy Assessment

4.3.1 Existing Land Cover Inventories and Atlases

The most previously studied and frequently avalanching areas within the park, (i.e. the JFS Canyon area and the GTSR) were intentionally not utilized to create training data to allow their use in accuracy assessments because they contain the most well-documented avalanche paths. Since training data were not truly random, out-of-bag statistics, cross validation, and relative classification errors do not suffice for the requirements in a standard accuracy assessment (Maxwell et al., 2018).

Accuracy assessments were calculated using the RMRS Raster Utility, and to assess model performance and the climatic influence of the Continental Divide, output classifications were separated on the east and west sides of the divide. Accuracies were compared for the 30%, 40%, and 50% thresholds (Appendix A). Assessments were made using validation datasets from prior field work, photo interpretation of prominent avalanche tracks, and from prior inventories listed in Table 5.

4.3.2 Digitized Avalanche Tracks

Prior inventories from Butler and Walsh (1990), Carrera (1990), and GNP's previous land-cover dataset (1999/2007) were consulted during the creation of a hand-

digitized avalanche dataset. The stark contrast in adjacent vegetation patterns between mature forest and the herb/shrub cover of avalanche tracks allows such tracks to be easily identified in ground-based and/or aerial photography (Butler & Walsh, 1990). Only segments which were clearly tracks were selected using the previously generated vectors from segmentation and the NAIP mosaics used in the classification. All segments were selected when viewed at a 1:2,500 scale. Selected segments were exported as vector shapefiles to produce an additional layer used for quantifying the disturbance based on image interpretation. Accuracy assessments were performed against this dataset (Appendix A Table 10).

5 RESULTS

5.1 Predicted Avalanche Track Locations

The 10 and 20% intervals had substantial errors based on visual assessment and comparison to prior inventories and were not further analyzed, yielding three land-cover datasets for further evaluation. The three different land-cover datasets for avalanche tracks at the 30%, 40%, and 50% probability thresholds are shown for the entirety of GNP in Fig. 5, and for five different regions of GNP in Figs. 6 through 10. Distinct tracks were missed by even the most accurate random forest prediction, particularly on northerly, shadowed aspects (Fig. 6). In certain southerly aspects, over-inclusion occurred (Fig. 7). Depending upon the probability threshold utilized, this analysis found between 5% to 12% of GNP's area to be avalanche tracks (Figure 11). This estimate excludes most starting zones and some runout zones because they spectrally differ compared to tracks, and were not included in training data. The locations of avalanche tracks provide a baseline spatial dataset for

quantifying and detecting change for this disturbance within the park. This and previous avalanche inventories are summarized in Table 5.

Inventory	Hectares	Acres	Year
Random Forest (RF) Land-Cover	20,405 – 52,649	50,424 – 130,100	2013
Digitized	11,443	28,277	2013
GNP Land-Cover "Avalanche-Burial Class"	19,808	48,949	1999/2007
Peitzsch and Fagre (Partial - GTSR)	2,120	5,241	No Date
RF Land-Cover (Partial – GTSR)	868	2,147	2013
Hamre and Overcast (Partial – JFS Canyon)	1,048	2,590	2004
RF Land-Cover (Partial - JFS Canyon)	964	2,383	2013

Table 5. Summary of avalanche track area mapped in each current and previous avalanche inventory, including partial atlases and land-cover classifications which contained an "avalanche burial path" category.

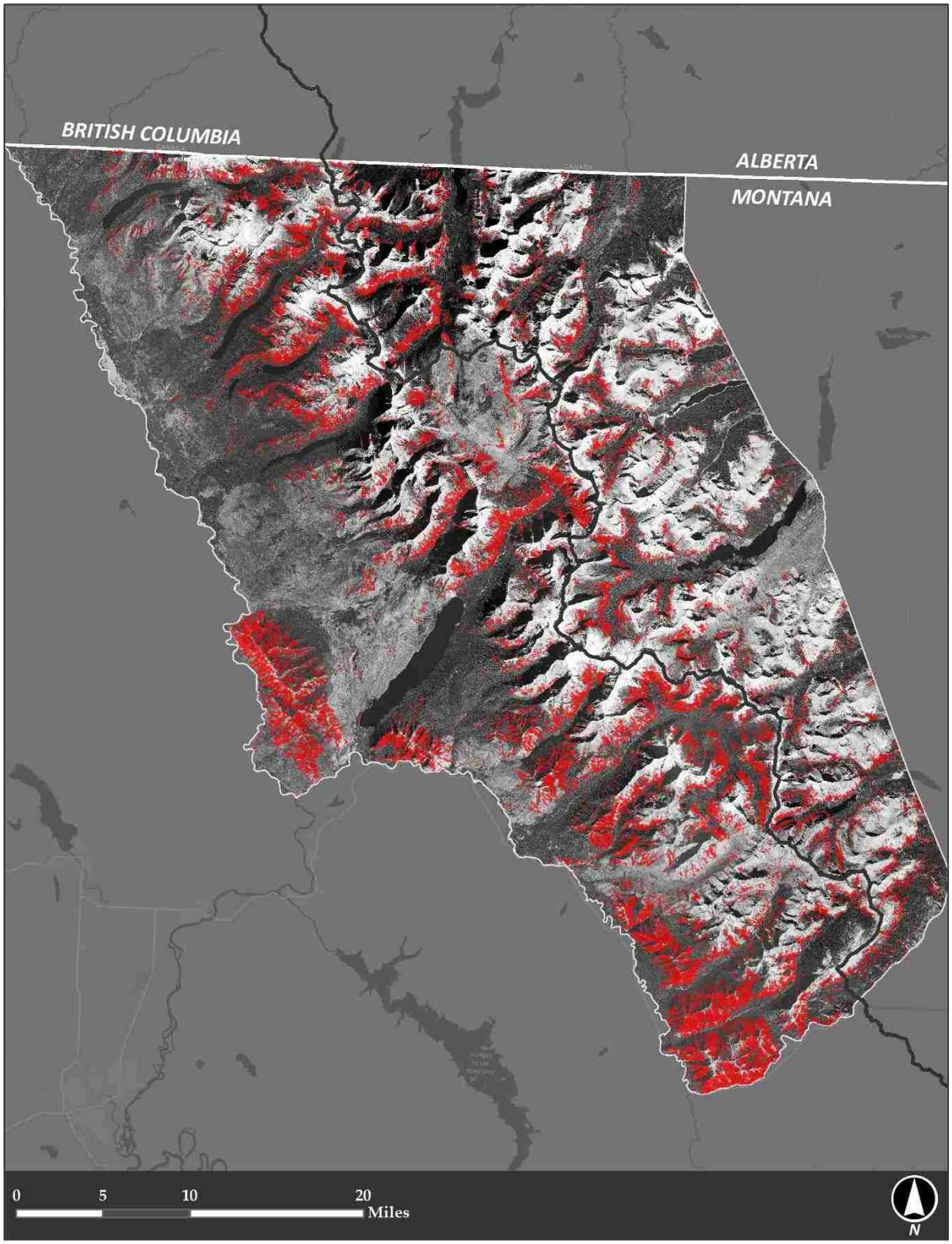

Figure 6. Map of the predicted avalanche track locations (red) using the 30% probability threshold from 500 iterations of a random forest algorithm and variables in Table 4. The Continental Divide is shown as a dark gray line.

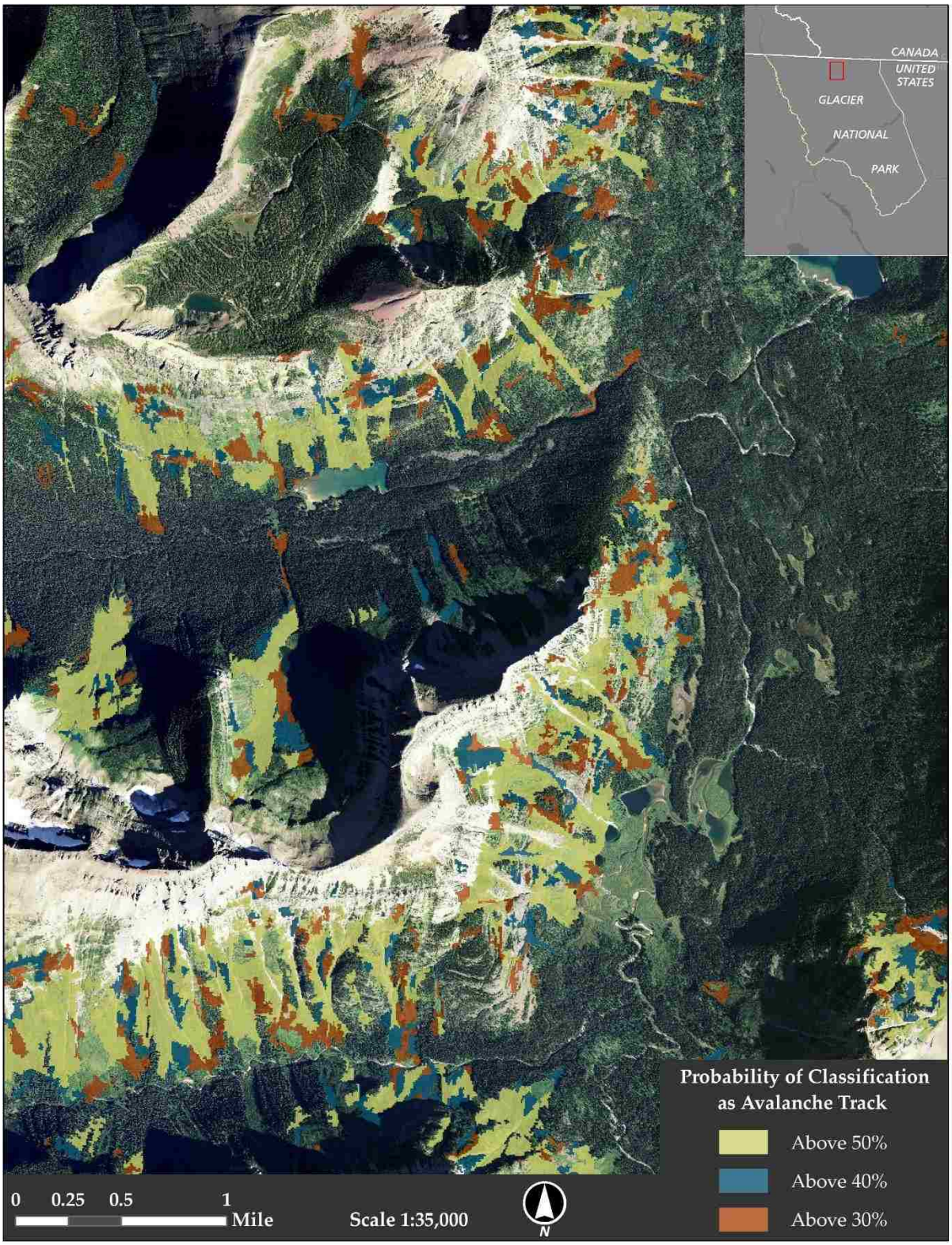

Figure 7. Map of the Goat Haunt area with avalanche tracks shown using 30%, 40%, and 50% probability thresholds.

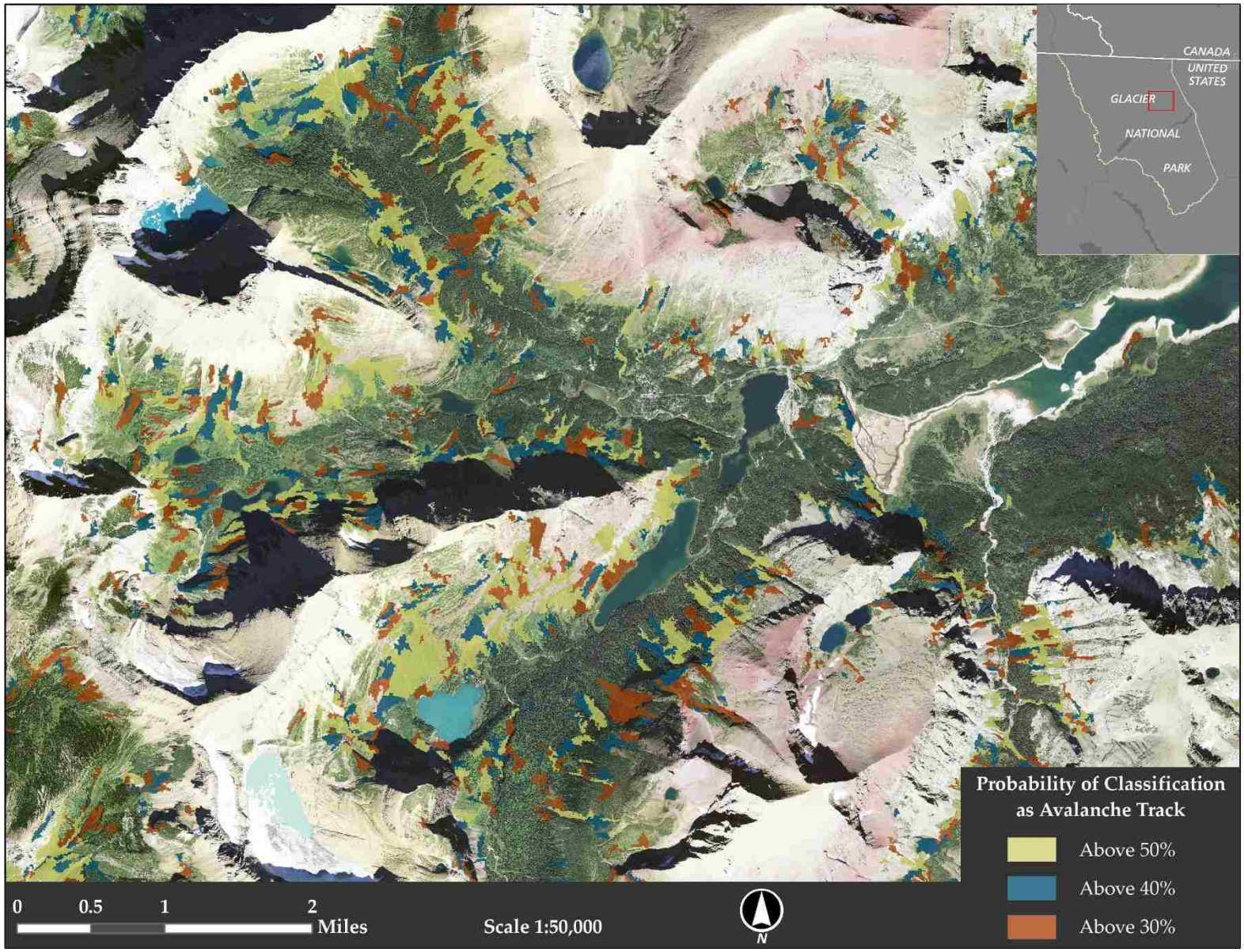

Figure 8. Map of the Many Glacier area with avalanche tracks shown using 30%, 40%, and 50% probability thresholds.

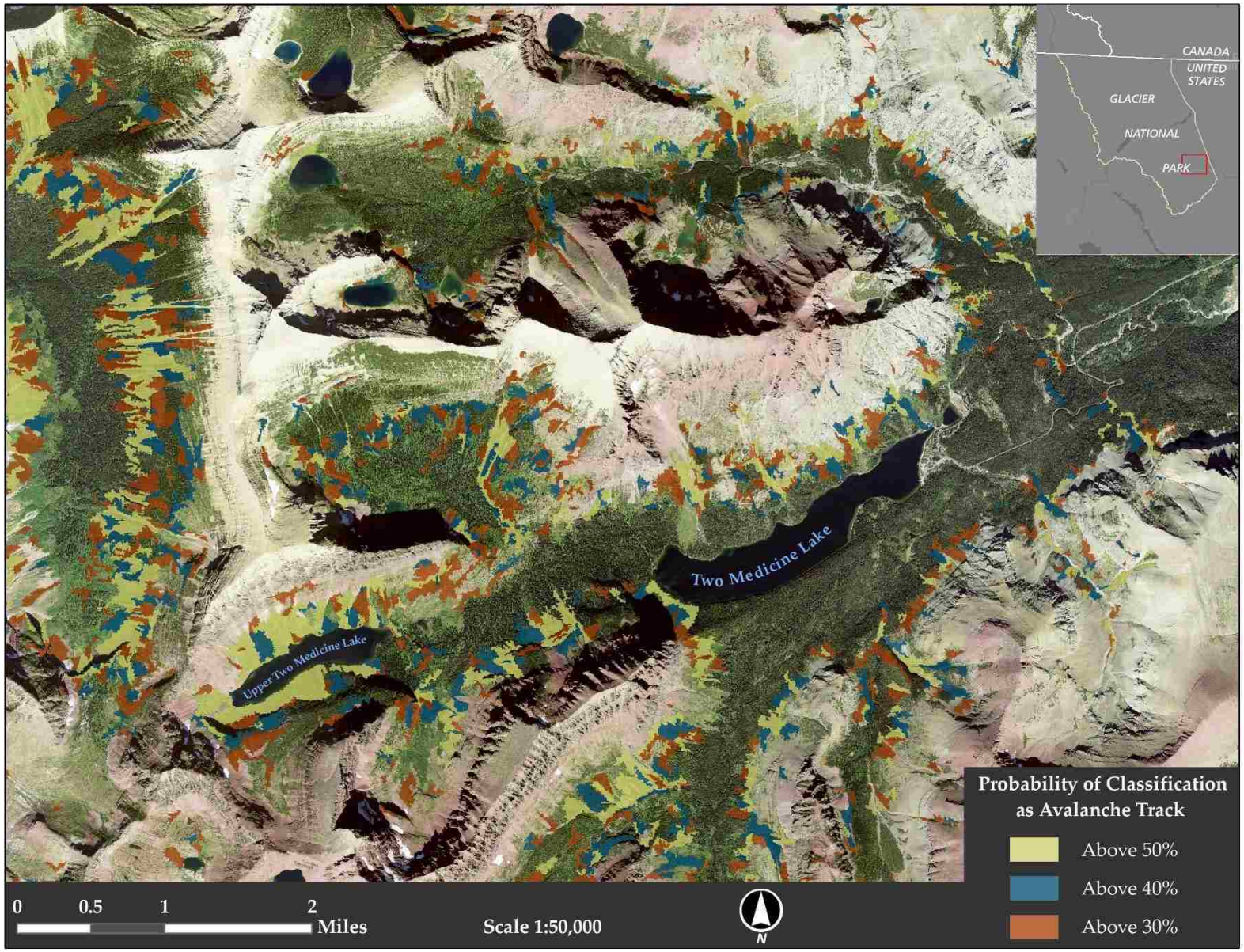

Figure 9. Map of the Two Medicine area with avalanche tracks shown using 30%, 40%, and 50% probability thresholds.

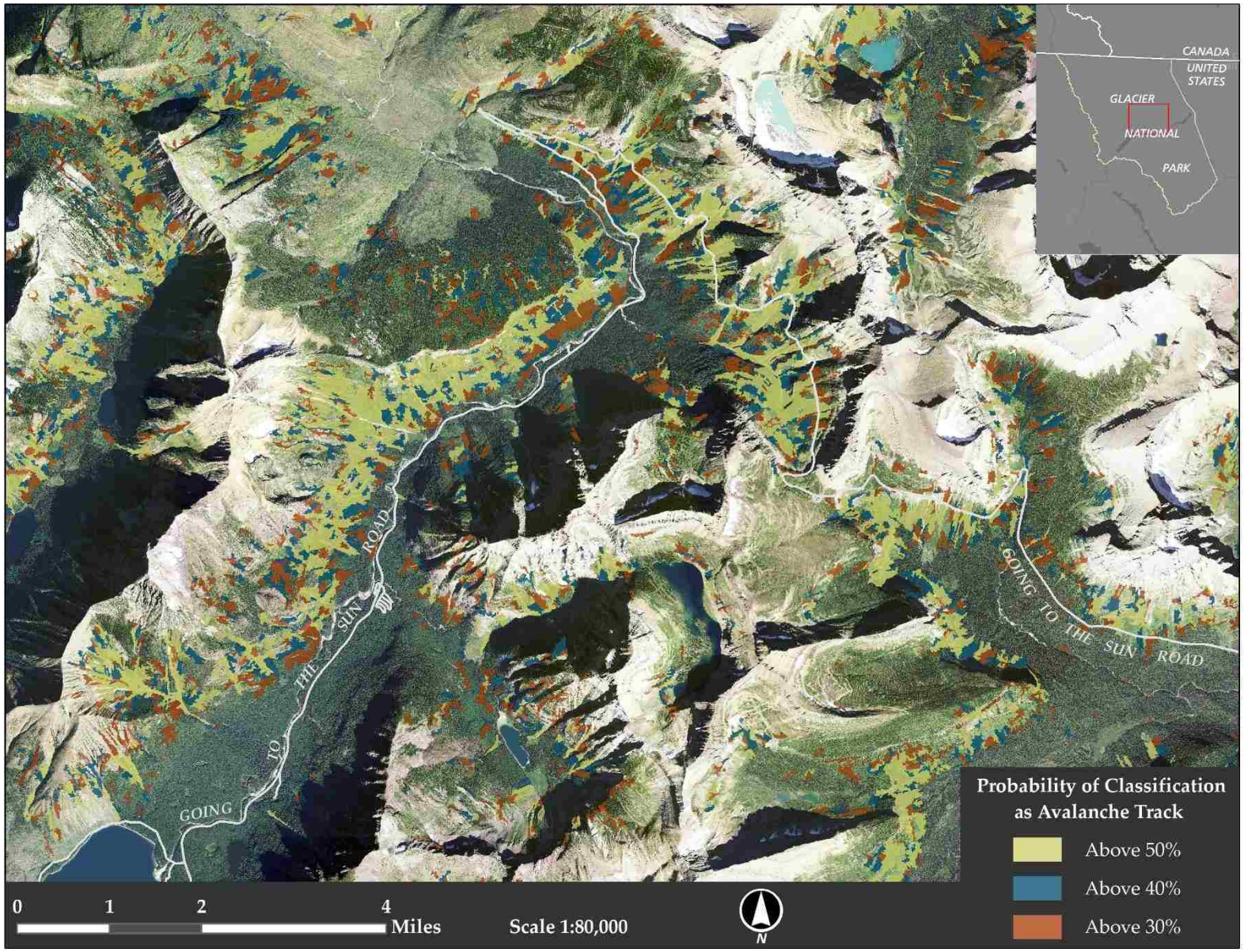

Figure 10. Map of the GTSR area with avalanche tracks shown using 30%, 40%, and 50% probability thresholds.

5.1.1 Overall Accuracy

The prediction using the 30% probability threshold most accurately mapped avalanche tracks based upon visual assessment and overall performance statistics (Fig. 6, Table 6). While the overall accuracy was 76%, the east and west sides of the divide differed substantially. The shrub/deciduous class tended to be the most confused with avalanche tracks, along with coniferous forest and burn scars. Confusion matrices are in Appendix A.

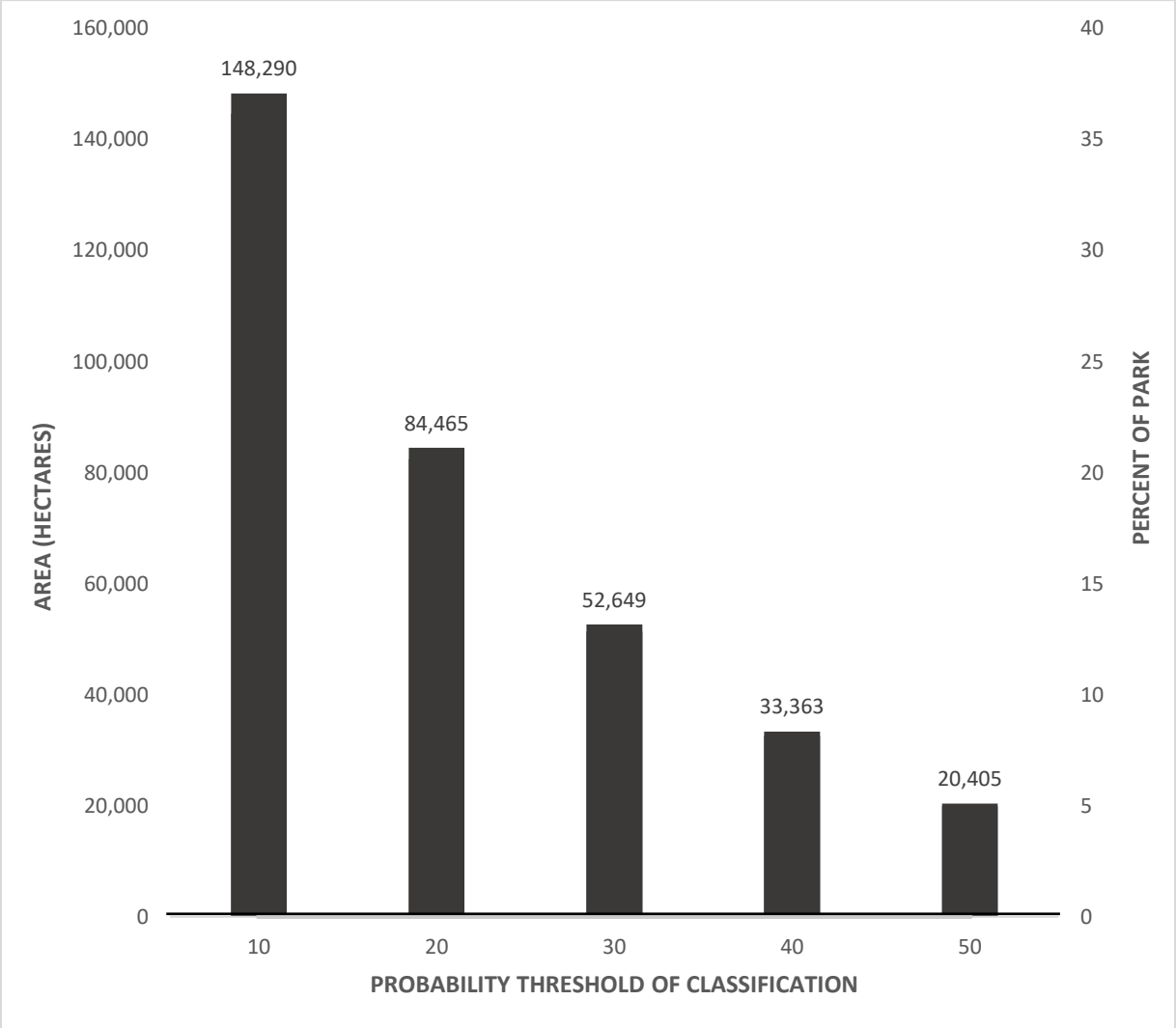

Figure 11. Area predicted as avalanche tracks using the 10%, 20%, 30%, 40%, and 50% class thresholds, from 500 random forest iterations on the selected variables (Table 4).

5.1.2 Probabilistic Thresholds

The western side of the continental divide contains substantially more avalanche tracks than the east side (Fig. 12, Table 6). Examples of each most likely class threshold (30%, 40%, and 50%) are in Figs. 13 through 15.

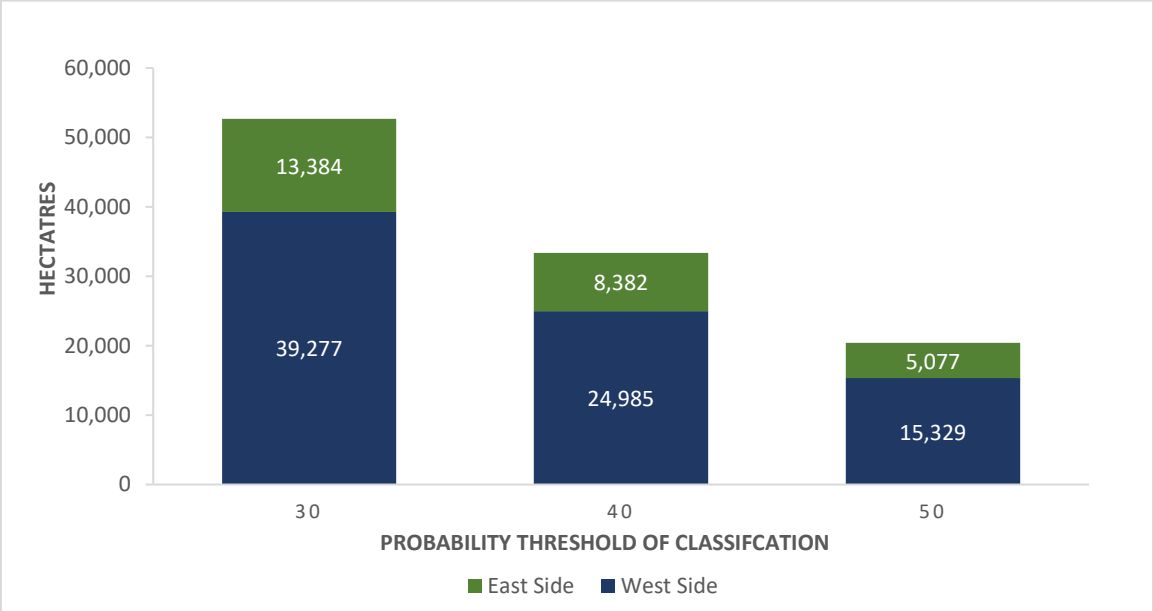

Figure 12. Area of predicted avalanche tracks on either side of the Continental Divide.

Threshold	Hectares	Acres	Percentage of Park	User Accuracy	Producer Accuracy	Overall Accuracy
10%	148,290	366,433	36.2	NA	NA	NA
20%	84,465	208,719	20.6	NA	NA	NA
30%	52,649	130,100	12.8	95%	62%	76%
40%	33,363	82,442	8.14	95%	56%	73%
50%	20,405	50,424	4.98	95%	55%	72%

Table 6. Estimates of avalanche track extent and overall, user, and producer accuracies for three avalanche track probability thresholds.

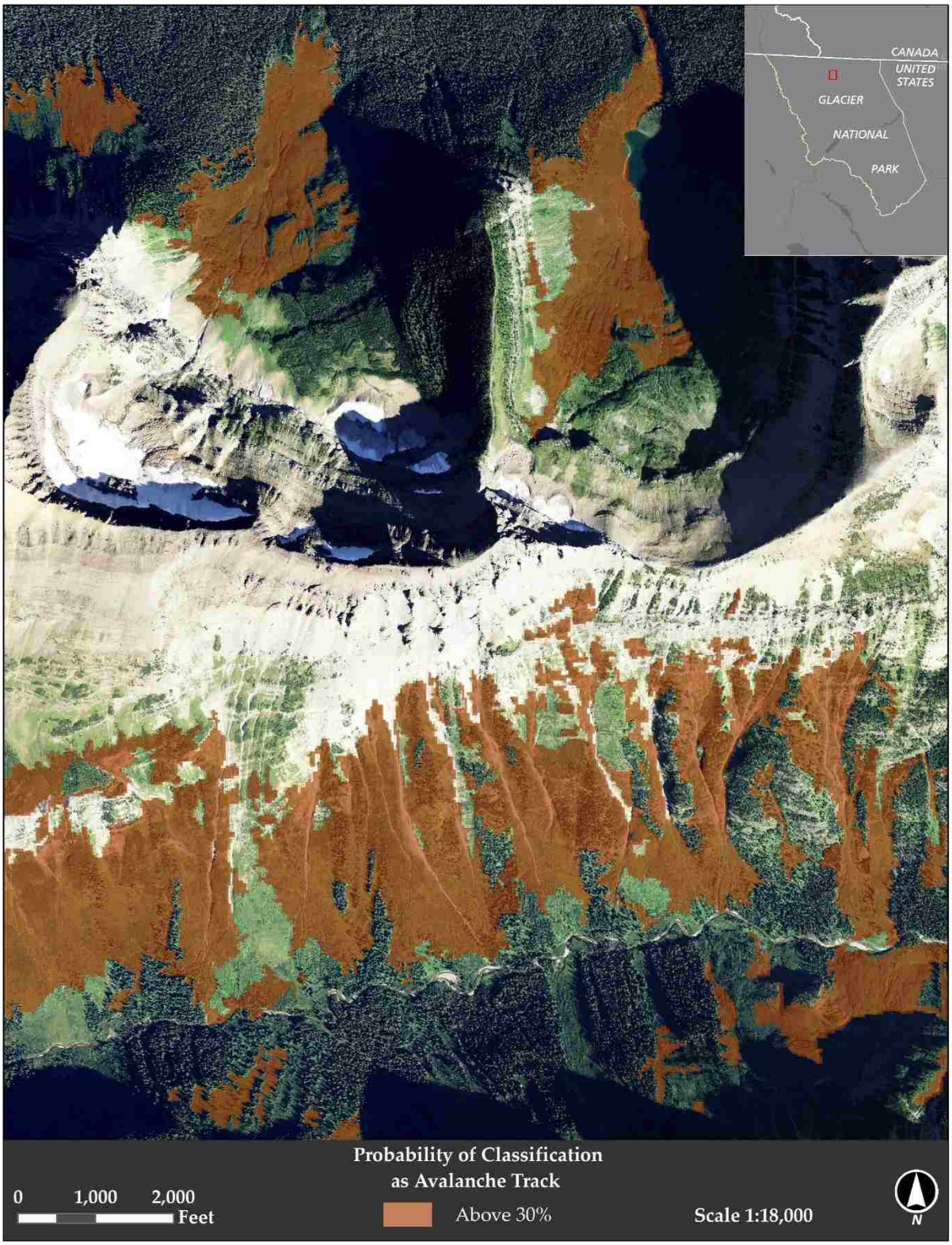

Figure 13. Tracks predicted at the 30% probability threshold from random forest algorithm near Waterton Lake.

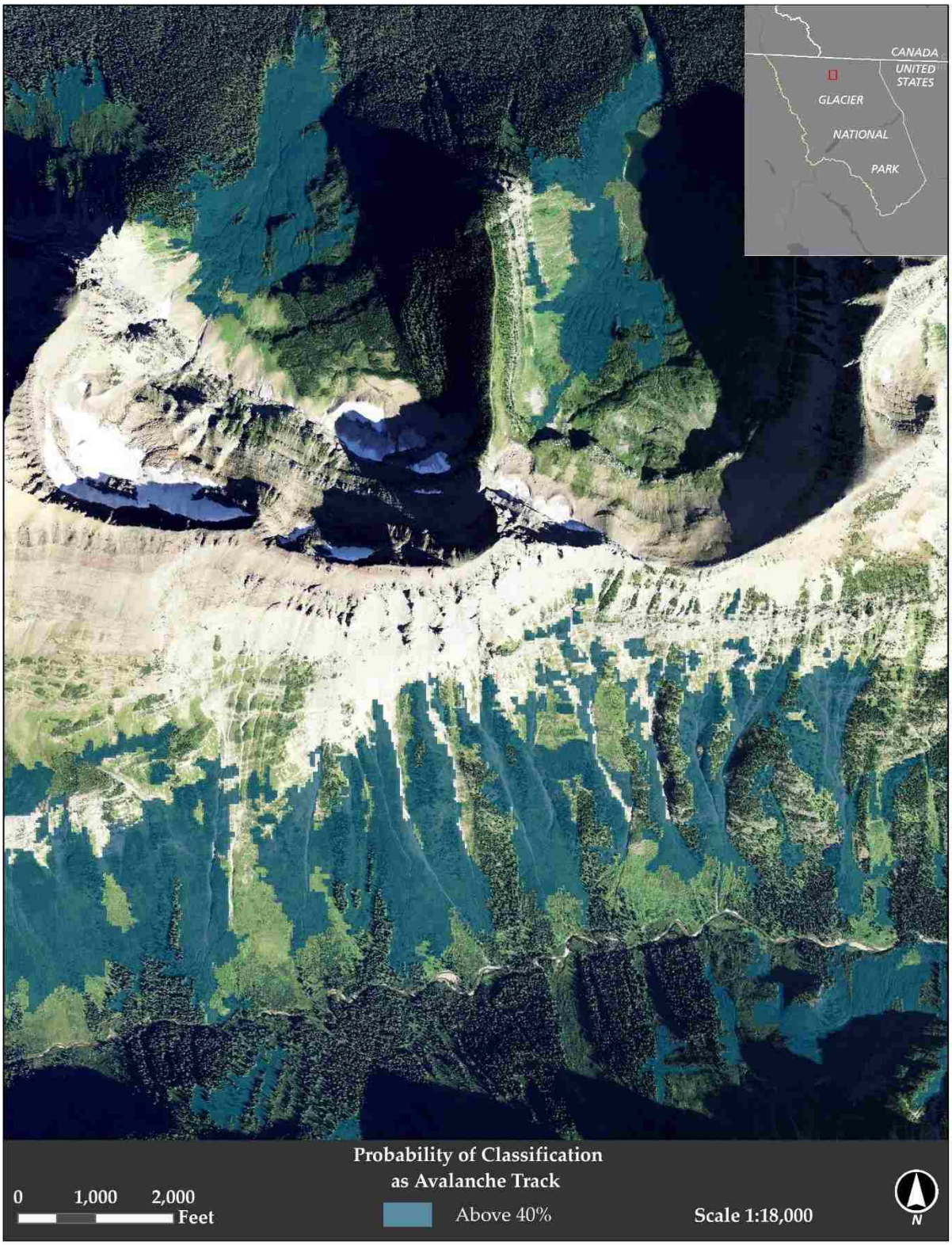

Figure 14. Tracks predicted at the 40% probability threshold from random forest algorithm near Waterton Lake.

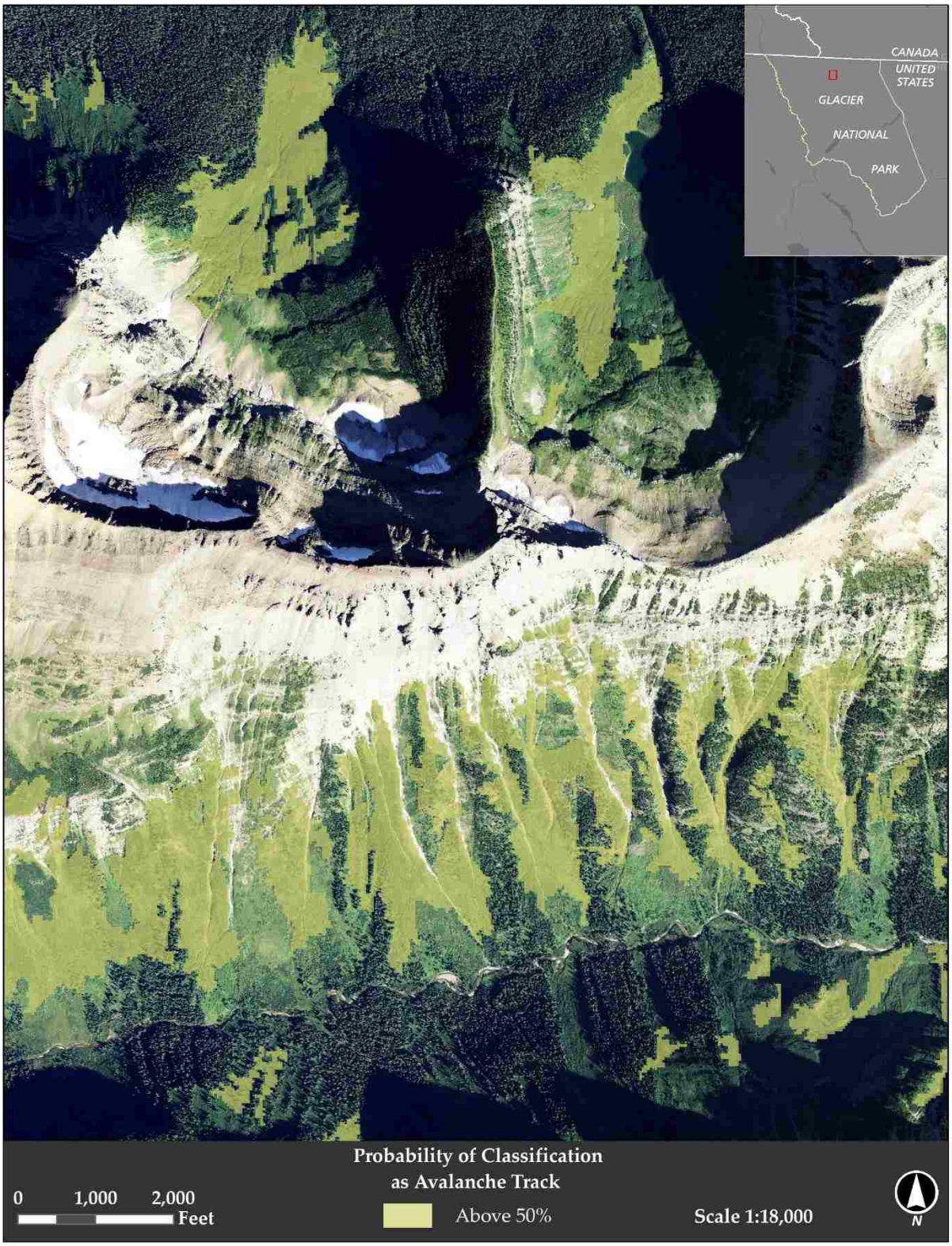

Figure 15. Tracks predicted at the 50% probability threshold from random forest algorithm near Waterton Lake.

5.1.3 Accuracy Assessments for Existing and Digitized Avalanche Inventories

Accuracy assessments for three probability thresholds of the most likely class being avalanche track (30%, 40%, and 50%) were conducted using the validation dataset created from prior inventories, field work, and photo interpretation. The 30% probability threshold achieved the highest accuracy at 76% (Appendix A, Table 1) and was used for further comparisons. In addition, predictions were assessed for east and west of the Continental Divide to examine model performance. Although more of a conservative estimation of predicted area due the exclusion of runout and starting zones, the digitized avalanche track dataset had 85% overall accuracy (Fig. 16; Table 10). The accuracy assessments for the park, and both sides of the continental divide at the 30% threshold are shown in Appendix A (Tables 1, 2, and 3).

While the accuracy for the overall park using the 30% threshold was 76%, the eastern side of the divide had a higher accuracy (82%), and the west side a lower accuracy (72%; Appendix A, Tables 2-3). Examples of predicted tracks compared to the prior GTSR and JFS Canyon atlases are shown in Figs. 17 and 18. Examining the differences in predicted tracks against inventory atlas paths reveal two very different types of mapping campaigns, one focusing on ecologic signature and one focusing on the entirety of the path, including starting zones at the top of the ridge.

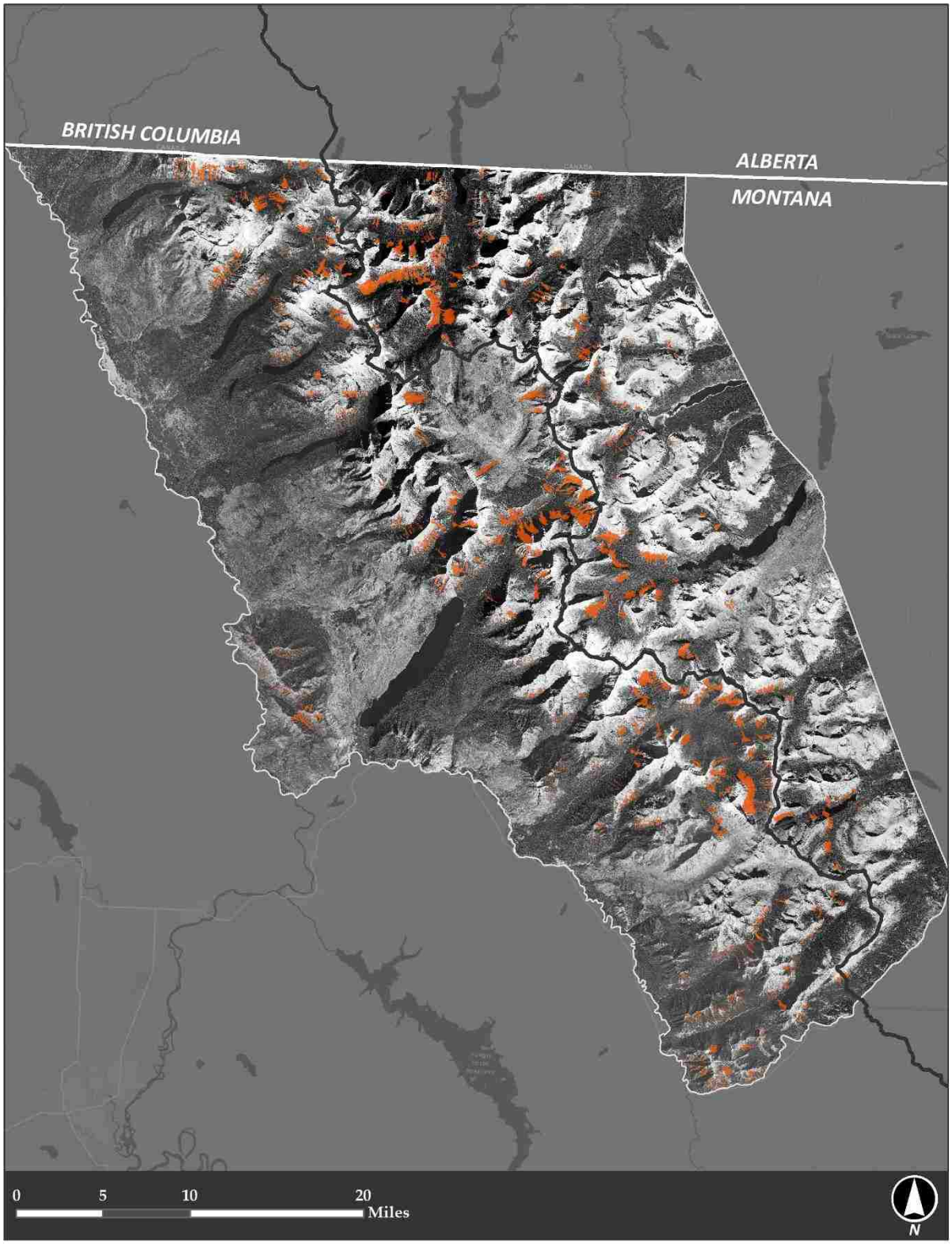

Figure 16. The image above displays the digitized avalanche track locations (orange) using photo interpretation, field visits, and prior land-cover data. The Continental Divide is shown in dark gray through the middle of the park.

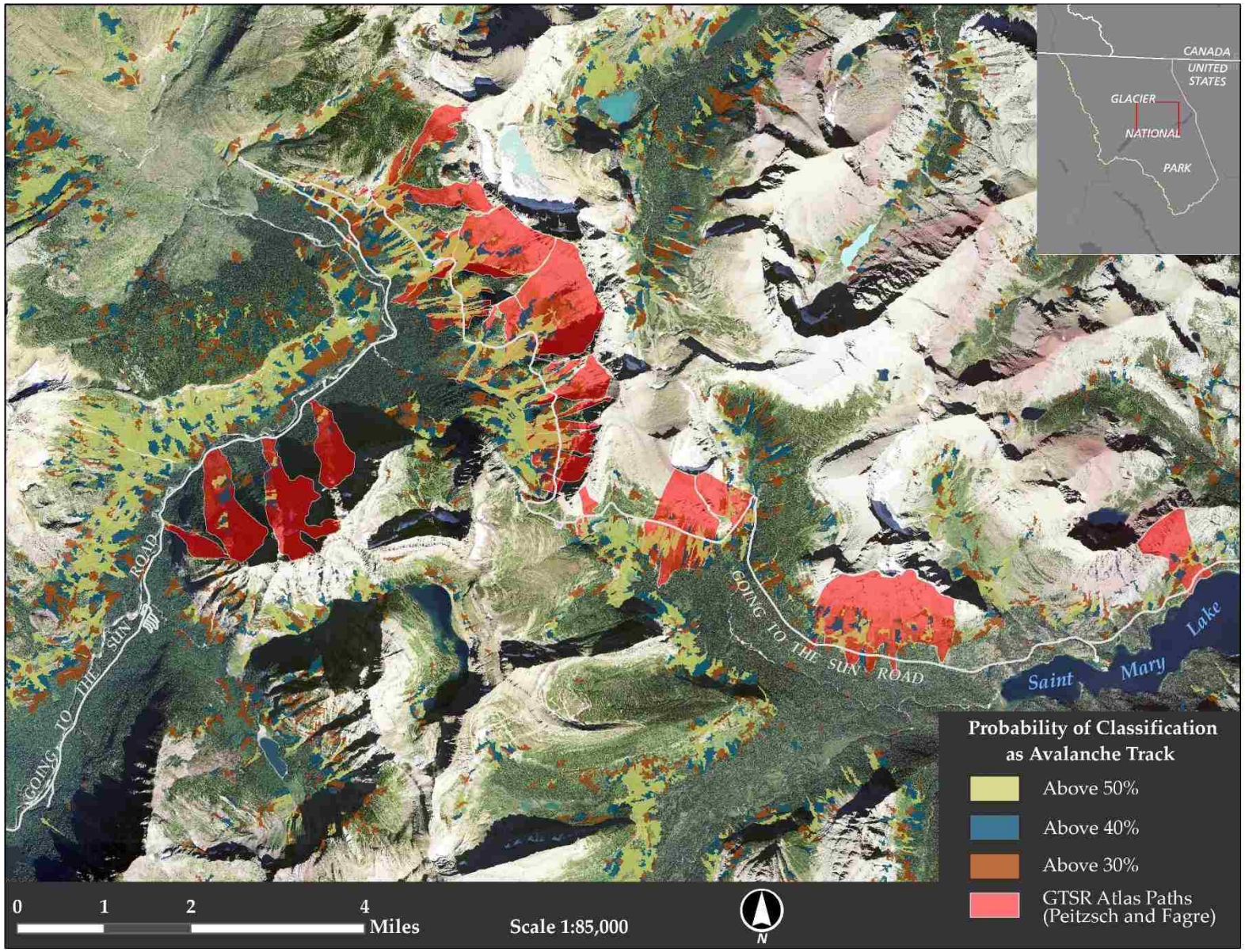

Figure 17. The GTSR Avalanche Atlas paths (bright red) from Peitzsch and Fagre (n.d) overlaid with predicted avalanche tracks at the three probability thresholds.

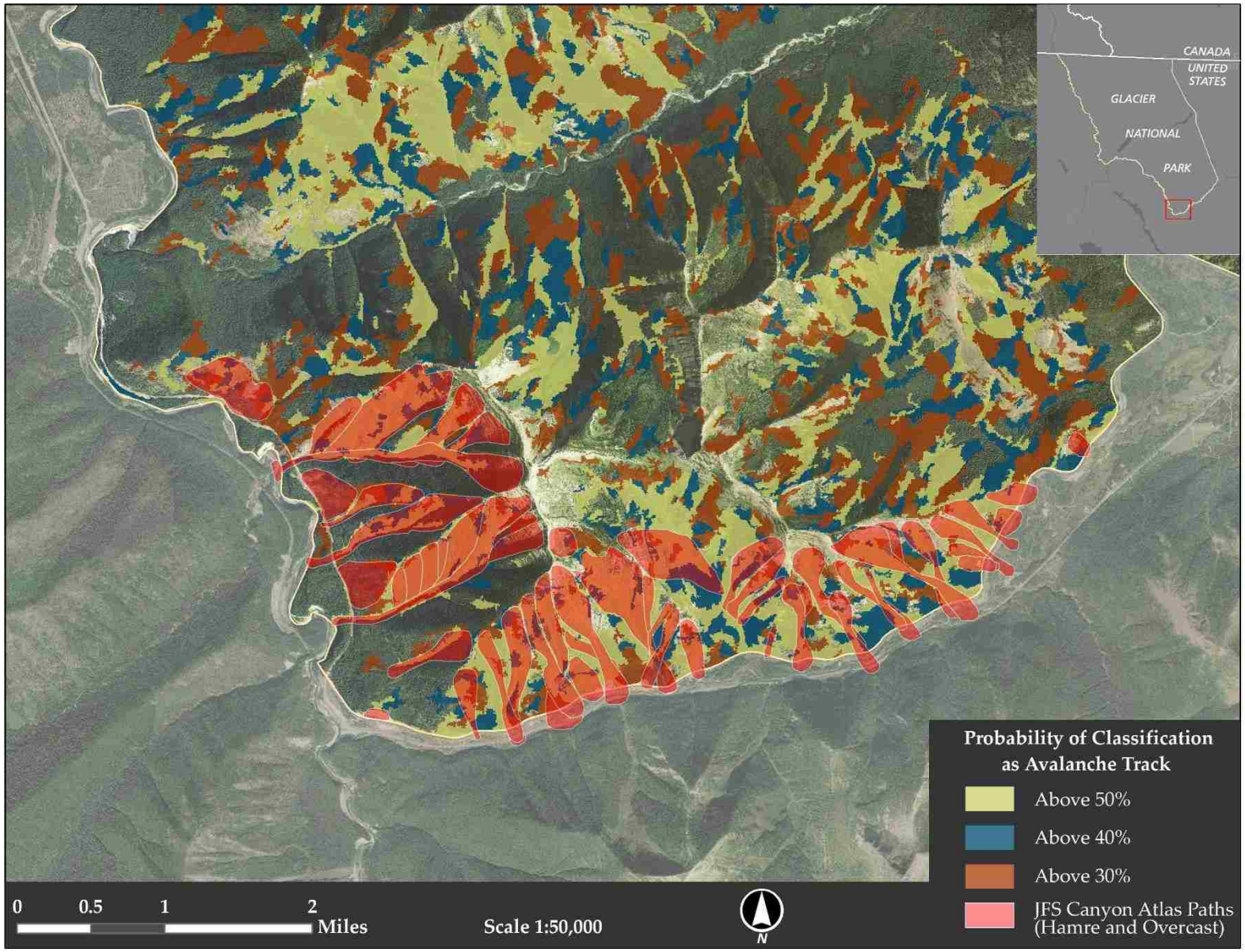

Figure 18. The JFS Canyon Avalanche Atlas paths (bright red) from Hamre and Overcast (2004) overlaid with predicted avalanche tracks at the three probability thresholds.

5.2 Geomorphic Characteristics

The avalanche tracks predicted at the 30% probability threshold were found on south and southeast facing slopes largely between 20° to 40° (Figs. 16-20). This was similar on either side of the divide, although the west side was predicted to have a much larger area of avalanche tracks while the east appears to have more area in the 20° to 35° range.

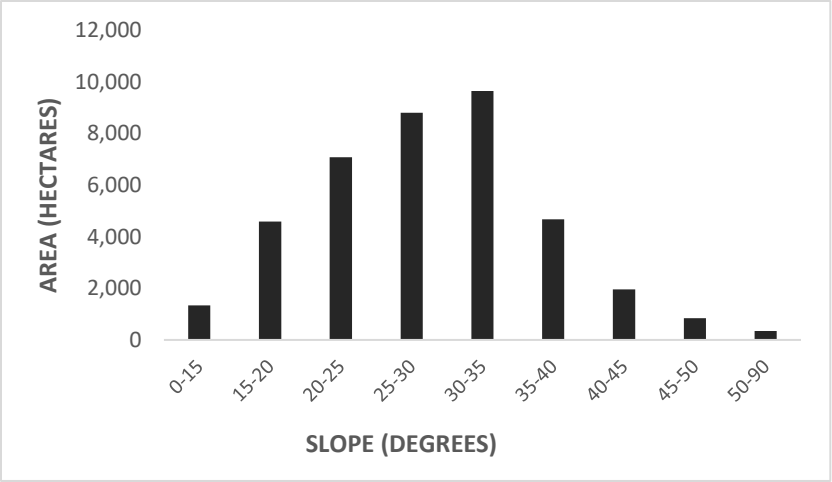

Figure 19. Mean slope of avalanche tracks predicted on the west side of the Continental Divide.

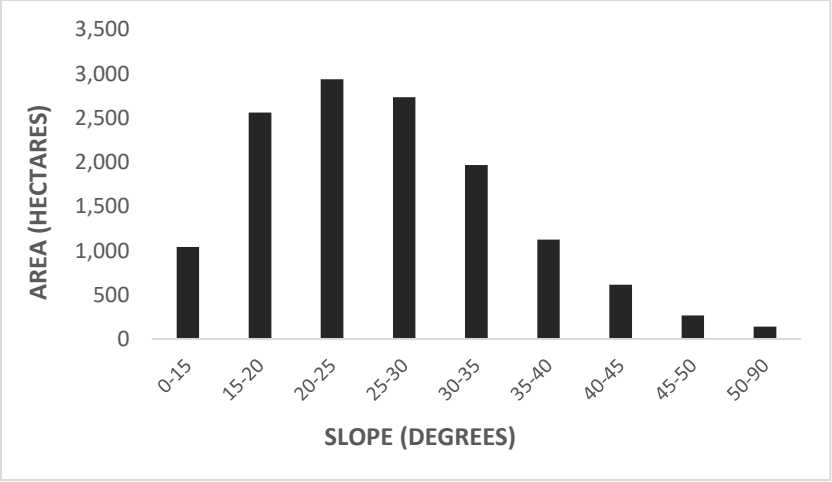

Figure 20. Mean slope of avalanche tracks predicted on the east side of the Continental Divide. Note the difference in y-axis compared to Fig. 19.

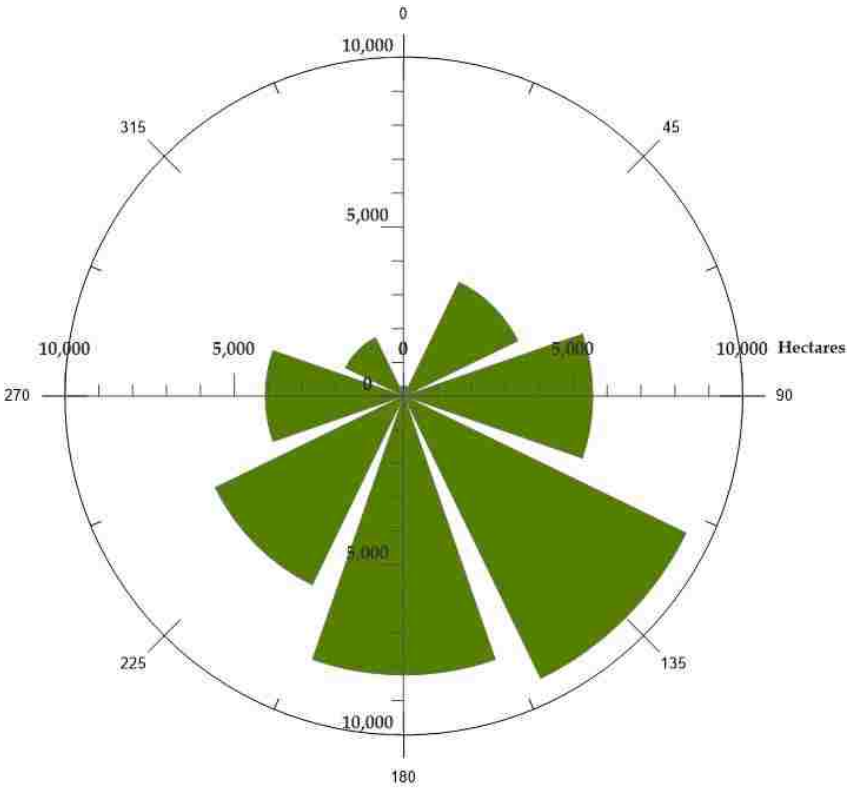

Figure 21. Aspect of avalanche tracks on the western side of the Continental Divide.

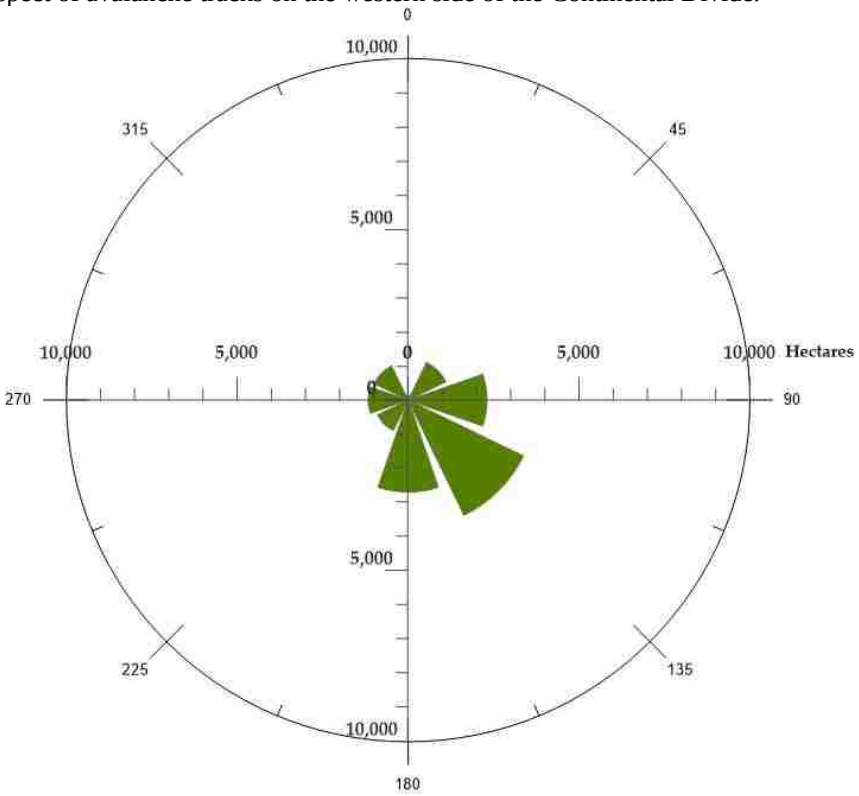

Figure 22. Aspect of avalanche tracks on for the east side of the Continental Divide.

5.3 Fire, Lakes, and Vegetation

Approximately 9,924 hectares (24,524 acres) or 18% of the predicted avalanche track corridors were in a fire-burn scar (Fig. 23). Of the 9,924 hectares, 69% of the predicted avalanche track areas were in burn scars from the 2003 fire year (Fig. 24). There is confusion in the accuracy assessments between regenerating forests and avalanche tracks (Appendix A, Tables 1-3). Fires younger than five years old are shown on the map, but were not considered because they occurred after the 2013 NAIP imagery was acquired.

In addition to avalanche tracks predicted in fire scars, many avalanche paths may possess the capability to transport material into or near lakes. Avalanches can transport debris flow, woody debris, and nutrients to bodies of water. Predicted tracks within 100 meters of a lake were mapped resulting in 776 hectares (1,919 acres) of avalanche tracks on the western side of the divide and 664 hectares (1,641 acres) on the eastern side of the divide (Fig. 25).

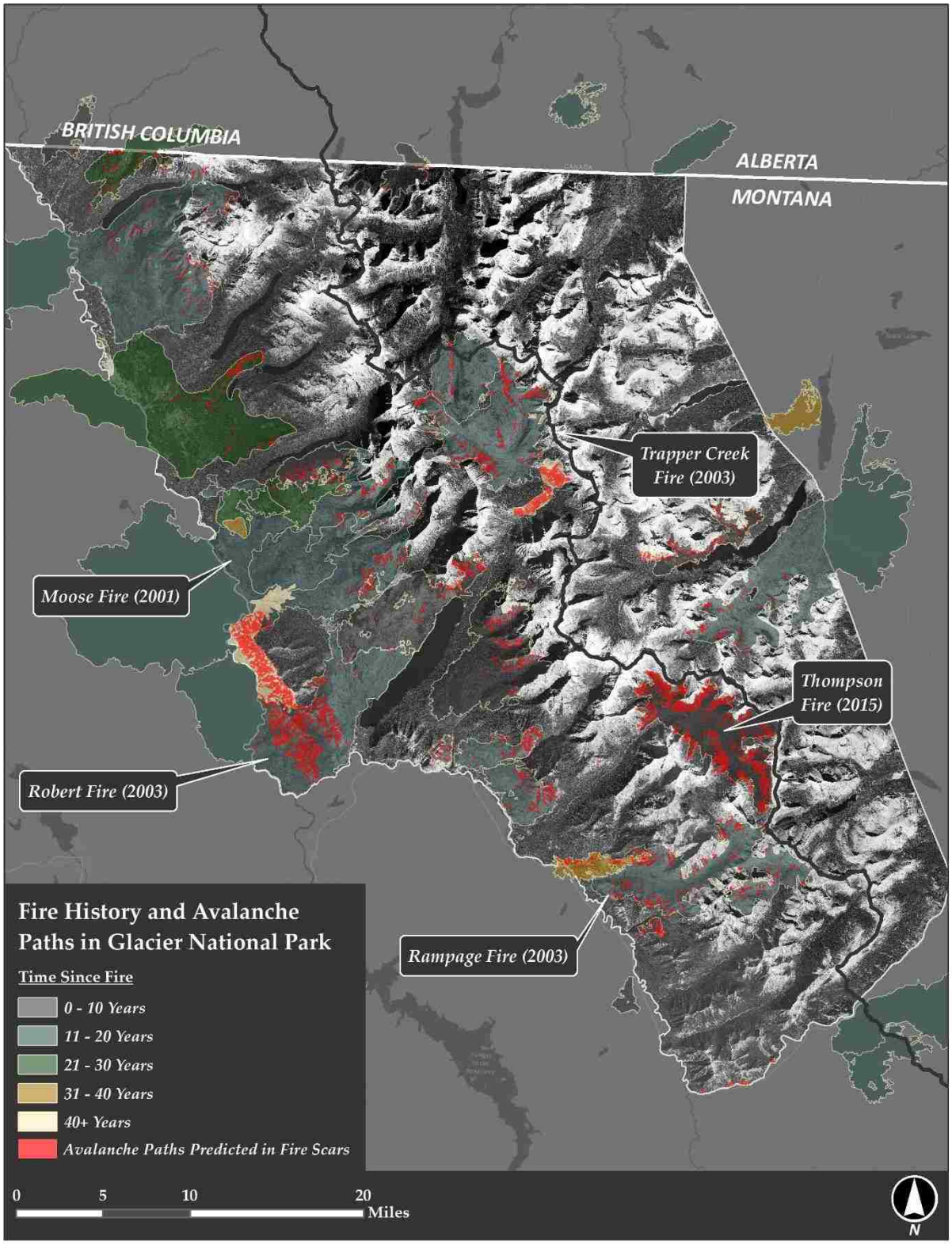

Figure 23. Map of predicted avalanche tracks (red) within recent fire scars in GNP. The Continental Divide is shown as a dark gray line.

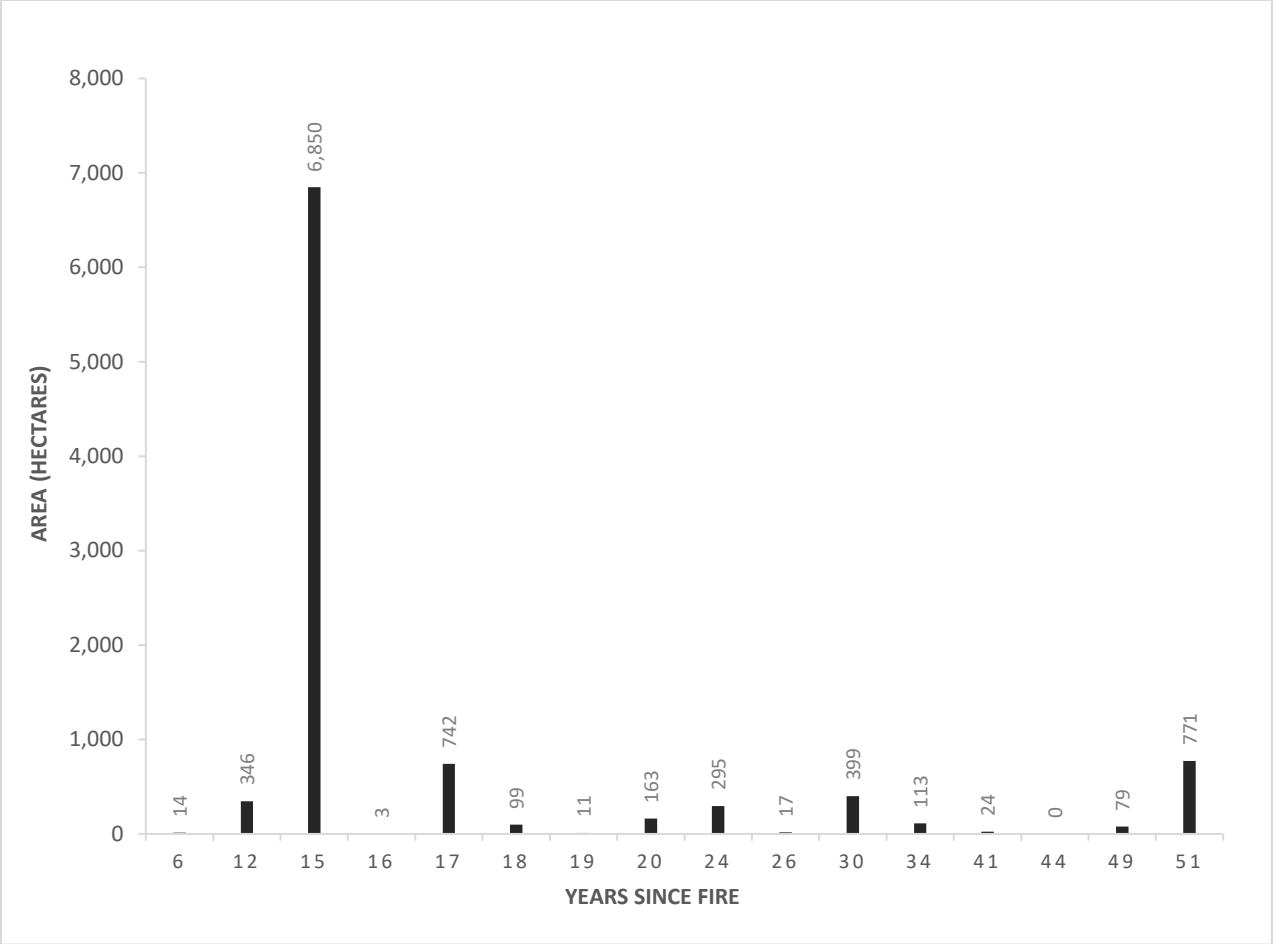

Figure 24. Graph of area of avalanche tracks within fire scars plotted against time since the fire. Fires less than five years old were excluded due to imagery acquisition in 2013.

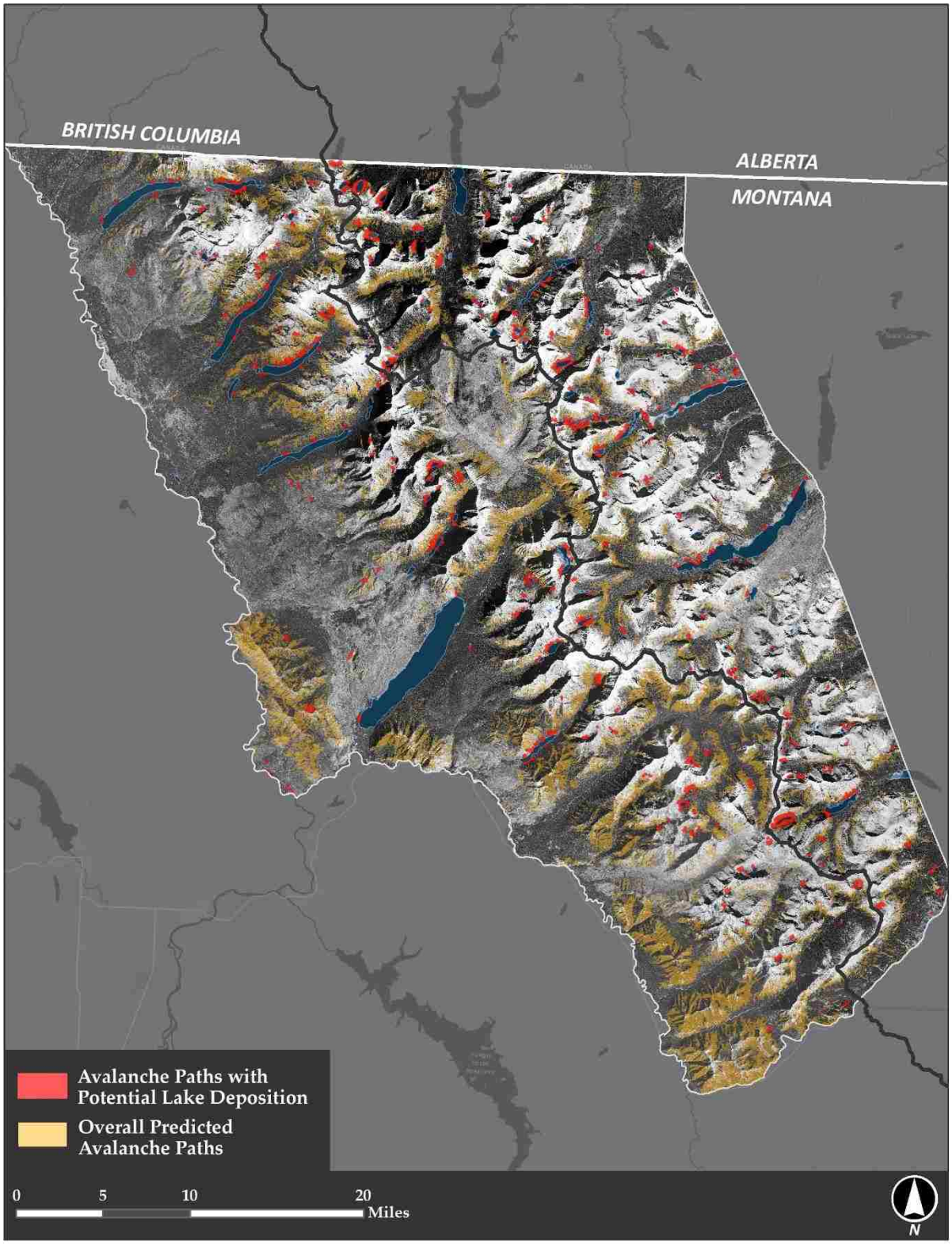

Figure 25. Map of avalanche tracks located within 100-meters of a lake (red) and predicted tracks in yellow. The Continental Divide is shown as a dark gray line.

6 DISCUSSION

6.1 Predicted Avalanche Track Heterogeneity and Model Accuracy

Over inclusion and exclusions existed within the maps of each probability threshold of avalanche tracks. Sampling and training data are crucial to the accuracy and performance of classifications. Random sampling implies that rarer land-cover classes (e.g. avalanche tracks), will be less represented overall, and it is common that classifications will under-predict less abundant classes relative to the true proportion of the land-cover class (Maxwell et al., 2018). Random sampling initially selected 9 segments as avalanche tracks compared to 26 for young forest/regeneration (Table 3). An equalized stratified sampling design was used to achieve an equal number of training samples for each class.

Out-of-bag (OOB) error in random forest models was calculated at 10% with accuracy of 90%. However, accuracy assessments of the 30%, 40%, and 50% probability thresholds revealed larger error estimates with accuracies between 72% to 76% (Appendix A, Tables 1, 4, and 7). The difference in error likely has to do with the use of segments, which are not fully statistically independent, leading to bias in the OOB error (Cánovas-García et al., 2017). Selecting additional training sites had the potential for imbalances in training data (Maxwell et al., 2018), however, this training data allowed the classifier to find significant patterns within the rarer land-cover class and differentiate it from the other land-cover categories.

Problems with overestimation and underestimation of tracks may be inherent from the heterogeneous nature of avalanche paths and their structure (Fig. 26) as well as the importance and influence of certain variables in random forest predictions. Confusion matrices indicated the most error between shrub classes and avalanche tracks, which are

spectrally similar since the vegetation is essentially the same (Fig. 27 and Appendix A, Tables 1-3). The floristic patterns of avalanche paths vary in structure based on the predominant type of avalanching (Malanson & Butler, 1986). Mapping strictly from vegetative and topographic data does not allow differentiation of fine-scale spatial patterns present in avalanche tracks. In theory, random forest modeling can decipher complex classes (i.e. the differences between shrubs on flat ground and shrubs on avalanche slopes) by finding patterns in slopes, aspects, and curvatures. However, based upon the variable classification errors and confusion matrices, confusion remained.

Shadow effects as well as the importance of variables such as elevation, PC2, PC3, and NDVI are probable contributors to modeling error. Attempts to reduce shadow effects by band ratios and PCA improved the results, but are so prominent in the steep topography of GNP that they could not be fully removed. The variance of elevation across the park is likely contributing to confusion as well; east and west of the divide elevations differ, perhaps causing confusion in pattern detection for the common elevations of avalanche tracks. Temporal limitations due to the dates of NAIP imagery used for this analysis also contributed to error. NAIP imagery from 2017 was recently released, however the dates of the imagery are much later in fall season than the 2013 year, resulting in many tracks with low NDVI values outside of peak greenness dates or tracks already covered in snow, making segmentation ineffective.

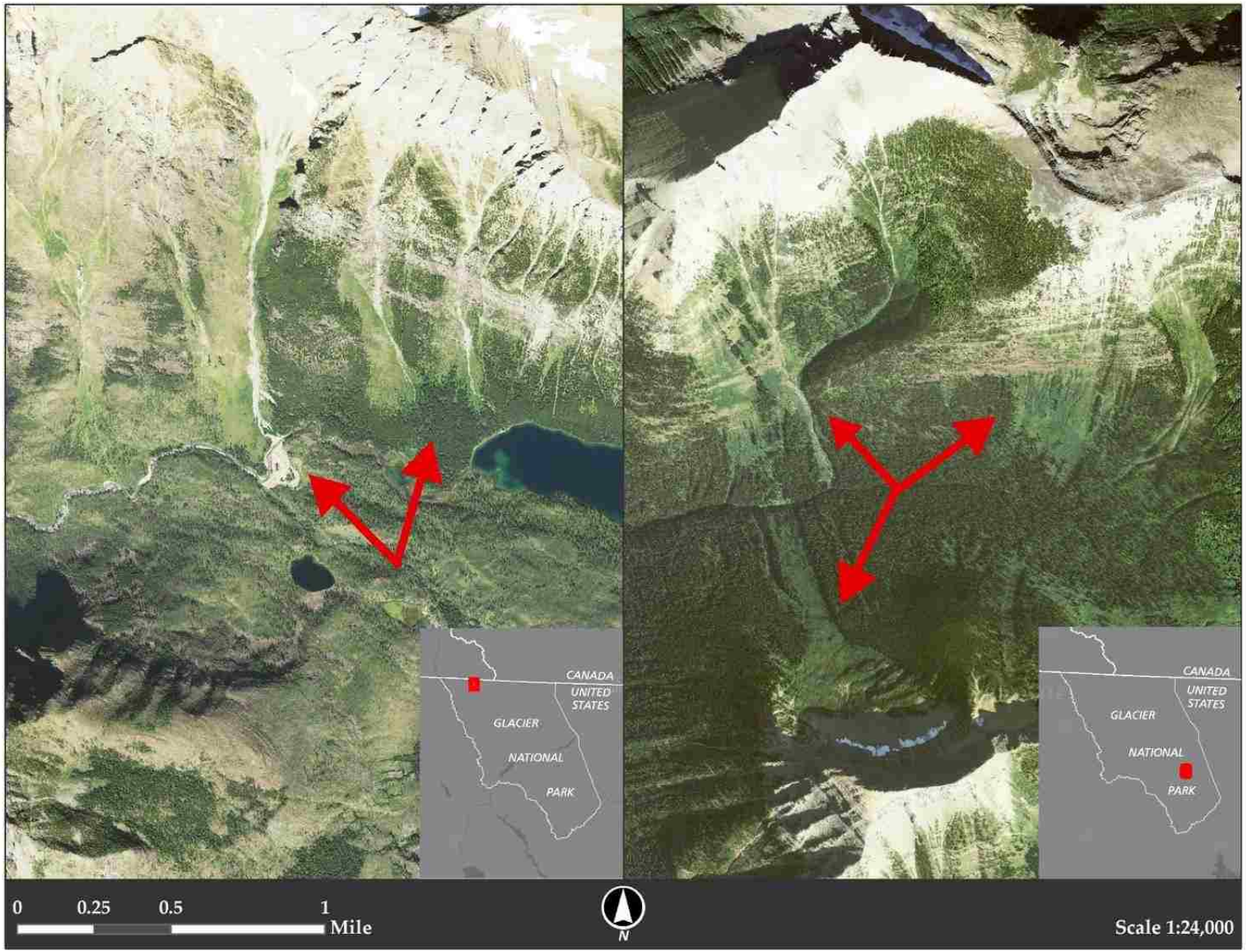

Figure 26. The red arrows illustrate two different avalanche paths with contrasting shapes, composition, and aspects, which might lead to spectral and algorithmic confusion.

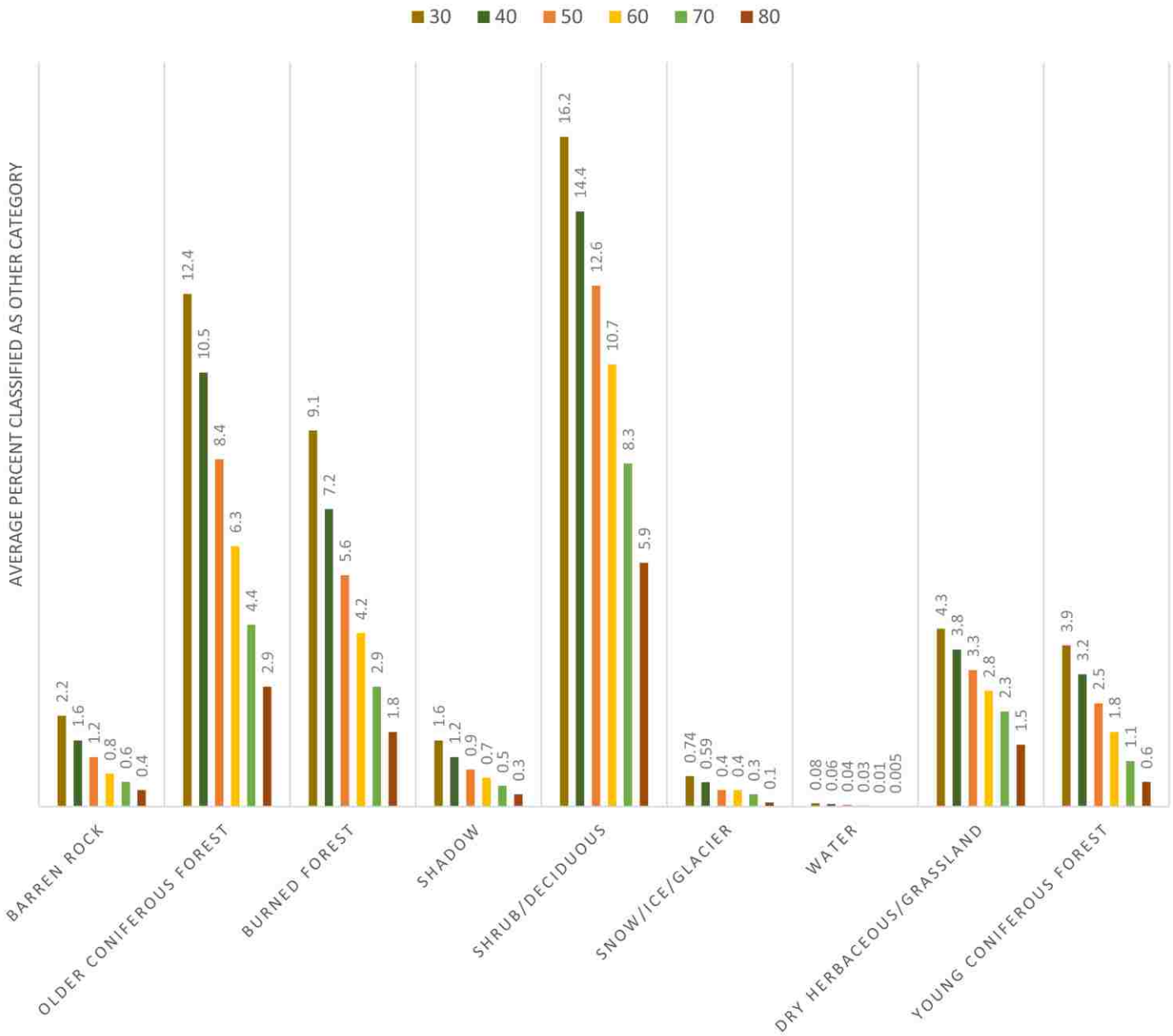

Figure 27 . Graph of the percentage of avalanche segments categorized into each of the other land-cover categories using the 30%, 40%, 50%, 60%, 70%, and 80% thresholds.

Accuracies on the western side of the Continental Divide were lower than the eastern side, but more avalanche track area was predicted on the west side (Fig. 12). The higher western predictions, however, are consistent with Butler's (1979) observations that avalanche paths are more concentrated in the west, in higher relief and areas receiving more precipitation.

6.2 Trends in Ecology and Geomorphology

6.2.1 Fire History and Compound Disturbance

In addition to shrubs and forbs being confused with avalanche tracks, coniferous forest and previous fire scars were consistently confused with avalanche tracks. The confusion between coniferous forests stems from a lack of spectral difference in the vegetation signatures between forest and avalanche track (maple, alder, fir, etc.) in GNP (Joint Fire Science Program, 2018). A considerable number of tracks were predicted in the Roberts Fire scar of 2003 while other inventories, such as Carrera's (1990) surficial geology map, and GNP's land-cover classification do not necessarily classify avalanche tracks within this area. With no documentation available for the occurrence of avalanche events or not, it is hard to describe if these areas actually are avalanching or are susceptible to future avalanche hazards. In a study on the post-fire avalanching, Germain et al. (2005) found a lack of synchronicity for avalanche events in disturbed versus undisturbed areas following disturbance events such as fire or logging, suggesting an increase in avalanche events is possible post-disturbance events.

The majority of avalanche tracks predicted in fire scars happen to be in fires from the 2003 fire season. The 2013 NAIP imagery was acquired 10 years after these fires, with the scars very visible in RGB imagery and the PCA. It is not likely that these burn scars

suddenly have an abundance of unknown avalanche tracks – rather it is likely that the development and regrowth of understory and regenerating forest stands are heavily contributing to spectral confusion with avalanche tracks in these areas.

Avalanche tracks predicted in fire scars may also indicate the potential for post-fire avalanche events. The prediction may be mapping avalanche susceptibility in certain areas, as with high severity fire there is commonly a loss of mature forest, in other words past tree anchors that may have inhibited avalanches in the past. It is possible that these burn scars are experiencing avalanche events, but do not fit the typical elongated track structure present in many of the other tracks in the park. Of particular interest may be the Thompson Fire from 2015 (Fig. 23), which appears to have predicted avalanche tracks, but occurred after the 2013 imagery acquisition. Newer imagery would be needed to effectively observe the changes in avalanche tracks in this location post-fire.

As fire frequency continues to increase all over the western U.S. (Flannigan et al., 2009), but with varying degrees of severity (Parks et al., 2016), research to study the advent of avalanching post-fire disturbance is a topic to be considered with climate change impacts. An area that may be of particular interest mapped with random forest modeling are the avalanche slopes below Stanton Mountain, an avalanching area in GNP near Lake McDonald. Following the Howe Ridge Fire in 2018, these avalanche slopes experienced the burning and torching of many trees, leaving unstable slopes. Future attention should be directed to the magnitudes of avalanches in this area this winter to examine any compound disturbances. With the loss of mature forest trim line on parts of the avalanche slopes, it is possible avalanche events will be able to extend farther than they previously have as it is possible for disturbances to interact with one another as one can trigger others (Paine et al.,

1998; Dale et al., 2001). Disturbance effects after high severity fires may prove to exhibit higher impacts of more frequent snow avalanching rather than the possible growth and decline of avalanching with changing alpine treelines.

6.2.2 Geomorphology

Tracks were consistently in south and south easterly aspects with slopes in potential (although not the most common) avalanche ranges at 20 to 40°. This is consistent with previous work describing possible avalanche terrain (McClung & Schaerer, 2006; Maggioni & Gruber, 2003; Armstrong & Williams, 1992) and previous geomorphic studies in the park (Butler, 1979; Butler & Walsh, 1990). The aspects also align with formally glaciated Pleistocene valleys, following the general topography of the park. While this could also be associated with error on the western side of the continental divide, the western patterns in aspect displayed a trend toward southwest aspects much more than the eastern side. It is also likely that the northerly aspect estimates are underrepresented, as even with image correction and the reduction of redundant information, notable tracks were still missed by modeling or shadow effects. The shadow effects are an unfortunate consequence of the steep topography in GNP and time of imagery acquisition.

Expansion of avalanching areas is already evident in the Little Granite avalanche track along the GTSR (Fig. 31; Fagre & Peitzsch, 2010), although contraction of tracks and regrowth of forest is illustrated in areas of the park (Figs. 28 and 29). Because the impact of changing snowpack on the frequency and magnitude of avalanches in high alpine environments, is inconclusive (Schneebeli et al., 1997; Bellaire et al., 2016), GNP will

continue to be an excellent environment to observe the impacts and potential changes of avalanche disturbance regimes due to its pristine, non-mitigating state.

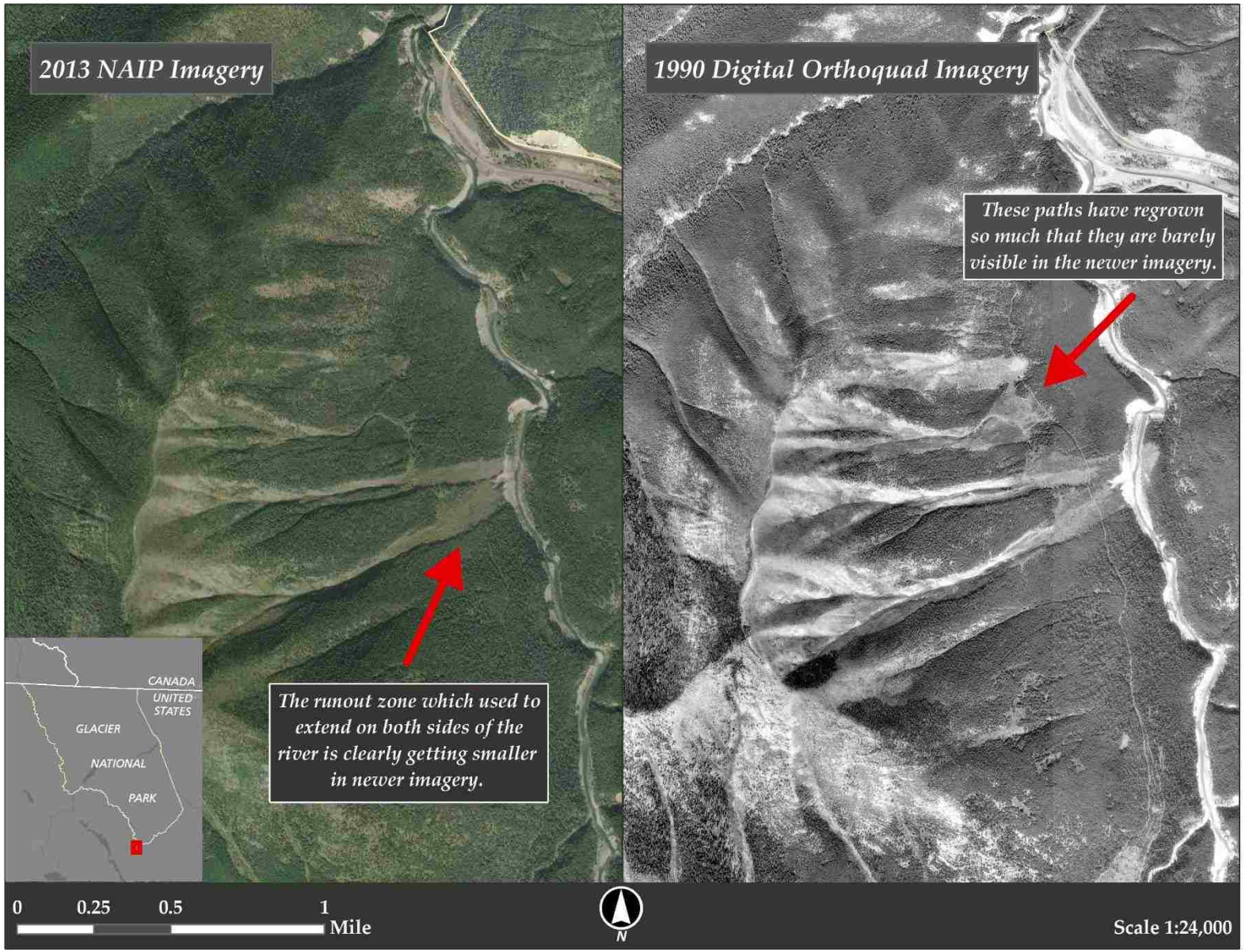

Figure 28. Although just outside the boundary of the park, the 2013 imagery (left) displays clear regrowth in the runout zones that extended much further in the 1990 imagery (right).

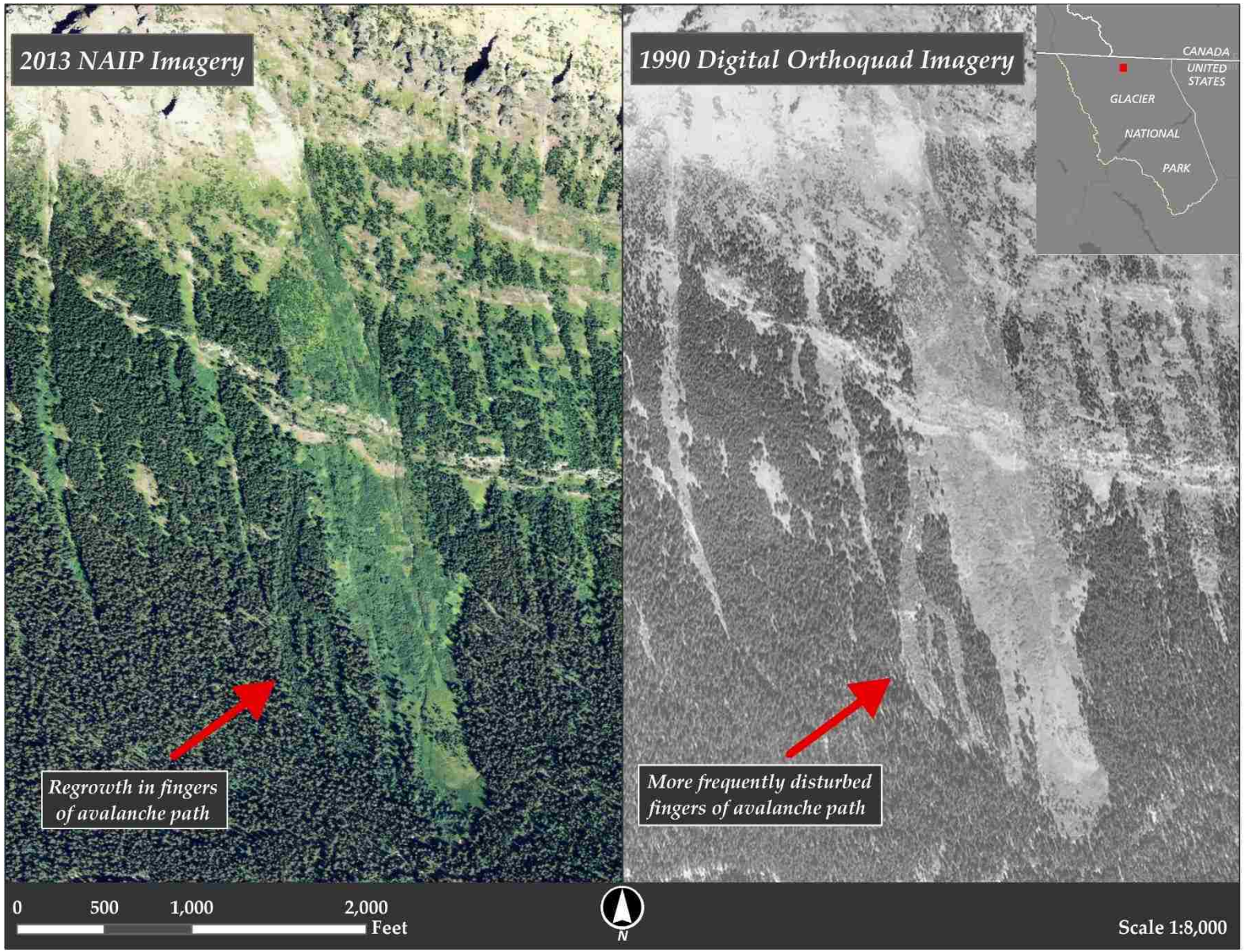

Figure 29. The 2013 imagery (left) displays regrowth of the previously disturbed fingers of the avalanche path which are much more prominent in the 1990 imagery (right) near Lake Janet.

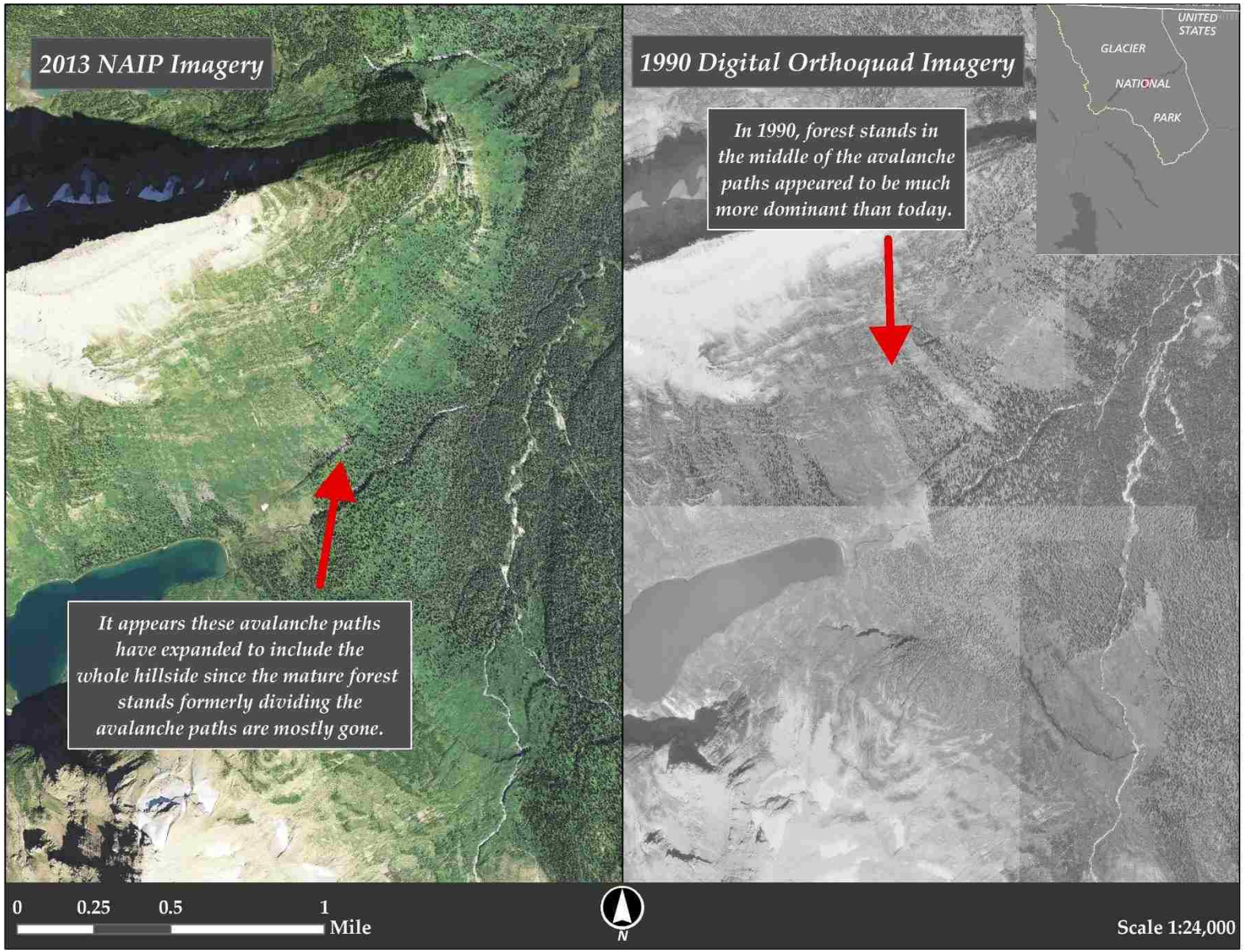

Figure 30. Avalanche paths near Gunsight Lake appear to be expanding, by way of disappearing forest stand between the paths.

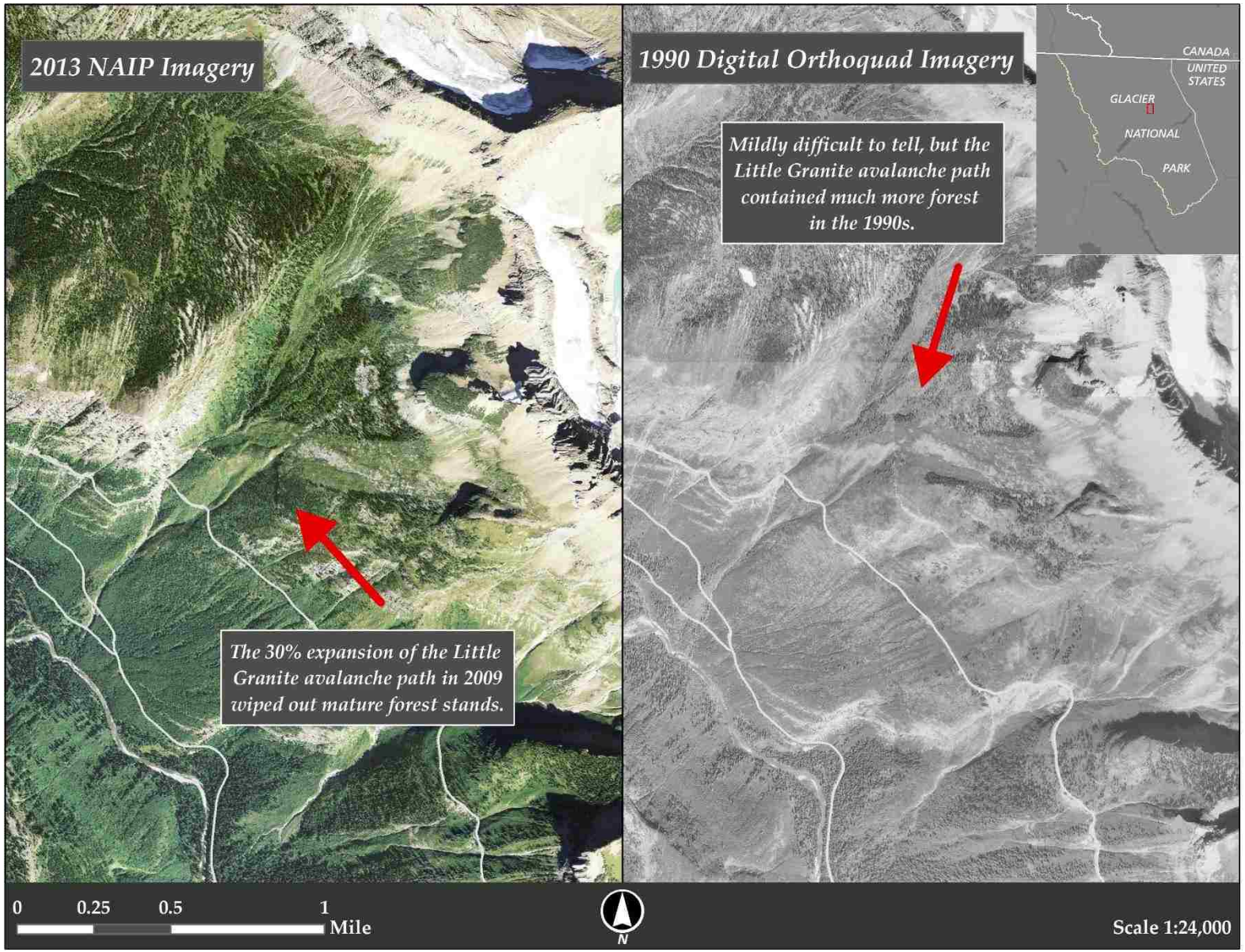

Figure 31. The results of a large magnitude event expanded the Little Granite avalanche path by 30% of its area, removing mature forest stands.

7 CONCLUSIONS AND FUTURE RESEARCH

7.1 Conclusions

This analysis found that 5%-12% of GNP consists of avalanche tracks, depending on choice of probabilistic threshold. This is consistent with past literature and provides a baseline inventory for quantifying this specific type of disturbance in the park. The avalanche tracks most hazardous to the public lie adjacent to the two main transportation corridors in the park, the GTSR and JFS Canyon. However, the abundance of avalanche tracks in GNP's more remote regions should not be dismissed, as they contribute to a common disturbance regime.

Probabilistic thresholds from 30% to 50% of a segment's most likely class being an avalanche track were evaluated. The 30% threshold had the highest accuracy at 76%. This methods offers a simple, yet effective and repeatable method to quickly map avalanche tracks over a large area using freely available data. Further analysis of this dataset found substantial differences in predicted avalanche track area on either side of the Continental Divide, consistent with previous work in avalanche climate studies in the park. In addition, this dataset also predicted avalanche tracks on south and southeast facing slopes, most frequently between 20° to 40°. These results were similar on either side of the divide, although the east appears to have a smaller area concentrated in the 30° to 35° range.

7.2 Suggested Future Research

With a baseline inventory of avalanche tracks in GNP available, time-series analysis could reveal if patterns occurring across the ecosystem, such as the contracting avalanche tracks shown in the Lake Janet and Middle Fork of the Flathead River areas or

the expanding avalanche tracks seen in the upper McDonald Creek and Gunsight Lake areas, are happening at similar rates or one is more common than the other. With changing fire regimes, more research on the changes in avalanche path size or post-fire avalanche frequency could aid in understanding ecologic trends.

Advancements in resolution, both spatial and temporal, of predictors could greatly enhance future classifications. For instance, LiDAR data exists in only the southern portion of the park, but if it existed for the entirety of GNP, tracks could be mapped based upon topography alone by examining gaps in tree canopy on specified slopes, similar to the techniques employed by Breschan et al. (2018). Acquisition of more recent imagery with perhaps more spectral bands (e.g. Sentinel-2) could also potentially detect some of the hard to distinguish trends in avalanche tracks as well, prompting room for further analyses.

REFERENCES

Ancey, C. (2016). Snow Avalanches. *Oxford Research Encyclopedia of Natural Hazard Science*. Oxford University Press. DOI: 10.1093/acrefore/9780199389407.013.17

Armstrong, B.R., & Williams, K. (1992). *The Avalanche Book*. Fulcrum Publishing.

Baatz, M., & Schäpe, A. (2010). Multiresolution segmentation: an optimization approach for high quality multi-scale image segmentation. 2000. *URL: http://www.agit. at/papers/2000/baatz_FP_12.pdf*.

Ballesteros-Cánovas, J. A., Trappmann, D., Madrigal-González, J., Eckert, N., & Stoffel, M. (2018). Climate warming enhances snow avalanche risk in the Western Himalayas. *Proceedings of the National Academy of Sciences*, *115*(13), 3410-3415.

Beers, T.W., Dress, P.E. & Wensel, L.C. (1966). Notes and observations: aspect transformation in site productivity research. *Journal of Forestry*, *64*(10), 691-692.

Bellaire, S., Jamieson, B., Thumlert, S., Goodrich, J. & Statham, G. (2016). Analysis of long-term weather, snow and avalanche data at Glacier National Park, BC, Canada. *Cold Regions Science and Technology*, *121*, 118-125.

Belgiu, M., & Drăguţ, L. (2016). Random forest in remote sensing: A review of applications and future directions. *ISPRS Journal of Photogrammetry and Remote Sensing*, *114*, 24-31.

Breiman, L. (2001). Random forests. *Machine Learning*, *45*(1), 5-32.

Breschan, J.R., Gabriel, A., & Frehner, M. (2018). A Topography-Informed Approach for Automatic Identification of Forest Gaps Critical to the Release of Avalanches. *Remote Sensing*, *10*(3), 433.

Butler D.R. (1979). Snow avalanche path terrain and vegetation, Glacier National Park, Montana. *Arctic and Alpine Research*, *11*(1), 17-32.

Butler D.R. (1986). Snow-avalanche hazards in Glacier National Park, Montana: meteorologic and climatologic aspects. *Physical Geography*, *7*(1), 72-87.

Butler, D.R., & Malanson, G.P. (1985). A history of high-magnitude snow avalanches, southern Glacier National Park, Montana, USA. *Mountain Research and Development*, 175-182.

Butler, D.R., & Sawyer, C.F. (2008). Dendrogeomorphology and high-magnitude snow avalanches: a review and case study. *Natural Hazards and Earth System Science*, *8*(2), 303-309.

Butler D.R., & Walsh S.J. (1990). Lithologic, structural, and topographic influences on snow-avalanche path location, eastern Glacier National Park, Montana. *Annals of the Association of American Geographers*, *80*(3), 362-378.

Cánovas-García, F., Alonso-Sarría, F., Gomariz-Castillo, F., & Oñate-Valdivieso, F. (2017). Modification of the random forest algorithm to avoid statistical dependence problems when classifying remote sensing imagery. *Computers & Geosciences, 103*, 1-11.

Carrara, P.E. (1990). *Surficial Geologic Map of Glacier National Park, Montana* (No. 1508-D).

Congalton, R.G., & Green, K. (2008). *Assessing the accuracy of remotely sensed data: principles and practices*. CRC press.

ESRI. (2018). ArcGIS Desktop: Release 10. Redlands, CA: Environmental Systems Research Institute.

Dale, V.H., Joyce, L.A., McNulty, S., Neilson, R.P., Ayres, M.P., Flannigan, M.D., et al., (2001). Climate change and forest disturbances: climate change can affect forests by altering the frequency, intensity, duration, and timing of fire, drought, introduced species, insect and pathogen outbreaks, hurricanes, windstorms, ice storms, or landslides. *BioScience*, *51*(9), 723-734.

Fagre D.B., & Peitzsch E.H. (2010). Avalanche ecology and large magnitude avalanche events, Glacier National Park, Montana, USA. *Proceedings 2010 International Snow Science Workshop*, October 17-22, Squaw Valley, California, 800-805.

Finklin, A. I. (1986). a climatic handbook for Glacier National Park-with data for Waterton Lakes National Park. *Gen. Tech. Rep. INT-GTR-204. Ogden, UT: US Department of Agriculture, Forest Service, Intermountain Research Station. 127p.*

Flannigan, M.D., Krawchuk, M.A., de Groot, W.J., Wotton, B.M., & Gowman, L.M. (2009). Implications of changing climate for global wildland fire. *International Journal of Wildland Fire*, *18*(5), 483-507.

Germain, D., Filion, L., & Hétu, B. (2005). Snow avalanche activity after fire and logging disturbances, northern Gaspé Peninsula, Quebec, Canada. *Canadian Journal of Earth Sciences*, *42*(12), 2103-2116.

Gökyer, E. (2013). Understanding landscape structure using landscape metrics. In *Advances in Landscape Architecture*. InTech.

Gorelick, N., Hancher, M., Dixon, M., Ilyushchenko, S., Thau, D., & Moore, R. (2017). Google Earth Engine: Planetary-scale geospatial analysis for everyone. *Remote Sensing of Environment*, *202*, 18-27.

Guan, H., Yu, J., Li, J., & Luo, L. (2012). Random forests-based feature selection for land-use classification using lidar data and orthoimagery. *International Archives of the Photogrammetry. Remote Sensing and Spatial Information Sciences*, *39*, B7.

Hamre, D., & Overcast, M. (2004). *Avalanche Risk Analysis, John Stevens Canyon, Essex, Montana*. Girdwood: Chugach Adventure Guides, 74p.

Hexagon Geospatial. (2018). ERDAS Imagine: Release 16. Madison, AL: Hexagon Geospatial.

Hogland, J., & Anderson, N. (2017). Function modeling improves the efficiency of spatial modeling using big data from remote sensing. *Big Data and Cognitive Computing*, *1*(1), 3.

Johnson, E.A. (1987). The relative importance of snow avalanche disturbance and thinning on canopy plant populations. *Ecology*, *68*(1), 43-54.

Joint Fire Science Program. (2018). *Spectral Library: Western Montana*. Retrieved from: https://www.frames.gov/assessing-burn-severity/spectral-library/western-montana

Kulkarni, A.D., & Lowe, B. (2016). Random forest algorithm for land cover classification. *Computer Science Faculty Publications and Presentations. Paper*, *1*.

Lillesand, T., Kiefer, R.W., & Chipman, J. (2014). *Remote Sensing and Image Interpretation*. John Wiley & Sons.

Luckman, B.H. (1977). The geomorphic activity of snow avalanches. *Geografiska Annaler. Series A. Physical Geography*, *59*(1-2), 31-48.

Luckman B.H. (1978). Geomorphic work of snow avalanches in the Canadian Rocky Mountains. *Arctic and Alpine Research*, *10*(2), 261-276.

Maggioni, M., & Gruber, U. (2003). The influence of topographic parameters on avalanche release dimension and frequency. *Cold Regions Science and Technology*, *37*(3), 407-419.

Malanson, G. P., & Butler, D. R. (1984). Transverse pattern of vegetation on avalanche paths in the northern Rocky Mountains, Montana. *The Great Basin Naturalist*, 453-458.

Malanson, G.P., & Butler, D.R. (1986). Floristic patterns on avalanche paths in the northern Rocky Mountains, USA. *Physical Geography*, *7*(3), 231-238.

Martinka, C.J. (1972). Habitat relationships of grizzly bears in Glacier National Park. *Montana. United States National Park Service, Glacier National Park, West Glacier, Montana, USA.*

Maxwell, A.E., Warner, T.A., & Fang, F. (2018). Implementation of machine-learning classification in remote sensing: an applied review. *International Journal of Remote Sensing*, *39*(9), 2784-2817.

McClung, D., & Schaerer, P. (2006). *The Avalanche Handbook*. The Mountaineers Books.

Paine, R.T., Tegner, M.J., & Johnson, E.A. (1998). Compounded perturbations yield ecological surprises. *Ecosystems*, *1*(6), 535-545.

Pal, M., & Mather, P.M. (2003). An assessment of the effectiveness of decision tree methods for land cover classification. *Remote Sensing of Environment*, *86*(4), 554-565.

Parks, S.A., Miller, C., Abatzoglou, J.T., Holsinger, L.M., Parisien, M.A., & Dobrowski, S.Z. (2016). How will climate change affect wildland fire severity in the western US? *Environmental Research Letters*, *11*(3), 035002.

Patten R., & Knight D. (1994). Snow avalanches and vegetation pattern in Cascade Canyon, Grand Teton National Park, Wyoming, U.S.A. *Arctic and Alpine Research*, *26*(1), 35-41.

Pederson, G.T., Reardon, B.A., Caruso, C.J., & Fagre, D.B. 2006. High resolution tree-ring based spatial reconstructions of snow avalanche activity in Glacier National Park, Montana, USA. In *Proceedings of the International Snow Science Workshop ISSW*, 436-443. Telluride CO.

Peitzsch E.H. & Fagre D.B. (n.d.). Going-to-the-Sun-Road, Glacier National Park, MT, USA: Avalanche Path Atlas. Northern Rocky Mountain Science Center, Technical Report, URL: http://nrmsc.usgs.gov/files/norock/research/GTSR_Avalanche_Atlas.pdf, accessed September 9, 2016.

Peitzsch, E.H., Hendrikx, J., & Fagre, D.B. (2015). Terrain parameters of glide snow avalanches and a simple spatial glide snow avalanche model. *Cold Regions Science and Technology*, *120*, 237-250.

Rapp A. (1960). Recent development of mountain slopes in Kärkevagge and surroundings, northern Sweden. *Geografiska Annaler*, *42*(2-3), 65-200.

Reardon, B.A., Fagre, D.B., & Steiner, R.W. (2004). September. Natural avalanches and transportation: A case study from Glacier National Park, Montana, USA. In *Proceedings of the International Snow Science Workshop*, 19-24.

Reardon, B.A., Pederson, G.T., Caruso, C.J., & Fagre, D.B. (2008). Spatial reconstructions and comparisons of historic snow avalanche frequency and extent using tree rings in Glacier National Park, Montana, USA. *Arctic, Antarctic, and Alpine Research*, *40*(1), 148-160.

Schläppy, R., Jomelli, V., Eckert, N., Stoffel, M., Grancher, D., Brunstein, D., & Deschatres, M. (2016). Can we infer avalanche–climate relations using tree-ring data? Case studies in the French Alps. *Regional environmental change*, *16*(3), 629-642.

Schneebeli, M., Laternser, M., & Ammann, W. (1997). Destructive snow avalanches and climate change in the Swiss Alps. *Eclogae Geologicae Helvetiae*, *90*(3), 457-461.

Schweizer, J., Jamieson, J. B., & Schneebeli, M. (2003). Snow avalanche formation. *Reviews of Geophysics*, *41*(4).

Steiner R.W., Dundas M., & Petri P. (2012). Interactive avalanche information system (IAIS). *Proceedings 2012 International Snow Science Workshop,* September 16-21, Anchorage, Alaska, 375-380.

Stoffel, M., Bollschweiler, M., Butler, D. R., & Luckman, B. H. (2010). Tree rings and natural hazards: an introduction. In *Tree Rings and Natural Hazards* (3-46). Springer, Dordrecht.

Trimble Geospatial (2018). eCognition: Release 1. Westminster, CO: Trimble, Inc.

Turner, M.G. (2010). Disturbance and landscape dynamics in a changing world. *Ecology*, *91*(10), 2833-2849.

Turner, G. M, Gardner, H. R., & O'Neill, V. R. (2001). Landscape Ecology in Theory and Practice, Springer-Verlag New York, Inc.

U.S. Geological Survey. (2007). *Spatial Vegetation Data for Glacier National Park Vegetation Mapping Project (2)* [ESRI Shapefile]. Denver, CO. Retrieved from: https://www.sciencebase.gov/catalog/item/542db539e4b092f17defca75

Walsh, S.J., Weiss, D.J., Butler, D.R., & Malanson, G.P. (2004). An assessment of snow avalanche paths and forest dynamics using Ikonos satellite data. *Geocarto International, 19*(2), 85-93.

APPENDIX A

		Visual Assessment										
Random Forest Prediction		Older Forest	Water	Snow/ Glacier	Shadow	Barren Rock	Burn	Shrub/ Deciduous	Young Forest	Dry Herb/ Grassland	Avalanche Track	UA
	Older Forest	98	0	0	0	0	0	1	7	0	23	76
	Water	0	88	0	0	0	0	0	0	0	0	100
	Snow/ Glacier	0	0	98	0	4	0	0	0	0	1	95
	Shadow	0	0	0	101	0	0	0	0	0	8	93
	Barren Rock	0	0	0	0	77	0	0	0	0	25	75
	Burn	0	0	0	0	4	88	0	0	5	85	48
	Shrub/ Deciduous	0	0	0	0	0	0	33	2	0	172	16
	Young Forest	5	0	0	0	0	0	2	60	0	1	88
	Dry Herb/ Grassland	0	0	0	0	0	1	4	0	44	11	73
	Avalanche Track	3	0	0	0	2	0	17	6	1	527	95
	PA	92	100	100	100	89	99	58	80	88	62	**76**

Table 1. Accuracy assessment for the 30% threshold for all of Glacier National Park. User's accuracy (UA) and producer's accuracy (PA) are in percentages. Overall accuracy in bold.

		Visual Assessment										
Random Forest Predication		Older Forest	Water	Snow/ Glacier	Shadow	Barren Rock	Burn	Shrub/ Deciduous	Young Forest	Dry Herb/ Grassland	Avalanche Track	UA
	Older Forest	51	0	0	0	0	0	1	1	0	10	81
	Water	0	42	0	0	0	0	0	0	0	0	100
	Snow/ Glacier	0	0	51	0	3	0	0	0	0	1	93
	Shadow	0	0	0	61	0	0	0	0	0	1	98
	Barren Rock	0	0	0	0	44	0	0	0	0	3	94
	Burn	0	0	0	0	2	30	0	0	1	29	48
	Shrub/ Deciduous	0	0	0	0	0	0	19	0	0	45	30
	Young Forest	4	0	0	0	0	0	1	10	0	0	67
	Dry Herb/ Grassland	0	0	0	0	0	0	1	0	5	2	63
	Avalanche Track	2	0	0	0	0	0	5	0	0	195	97
	PA	89	100	100	100	90	100	70	91	83	68	**82**

Table 2. Accuracy assessment for the 30% threshold for east of the Continental Divide in Glacier National Park. Overall accuracy in bold.

		Visual Assessment										
Random Forest Prediction		Older Forest	Water	Snow/ Glacier	Shadow	Barren Rock	Burn	Shrub/ Deciduous	Young Forest	Dry Herb/ Grassland	Avalanche Track	UA
	Older Forest	47	0	0	0	0	0	0	6	0	13	71
	Water	0	46	0	0	0	0	0	0	0	0	100
	Snow/ Glacier	0	0	47	0	1	0	0	0	0	0	98
	Shadow	0	0	0	40	0	0	0	0	0	7	85
	Barren Rock	0	0	0	0	33	0	0	0	0	22	60
	Burn	0	0	0	0	2	58	0	0	0	56	50
	Shrub/ Deciduous	0	0	0	0	0	0	14	2	0	127	10
	Young Forest	1	0	0	0	0	0	1	50	0	1	94
	Dry Herb/ Grassland	0	0	0	0	0	1	3	0	39	9	75
	Avalanche Track	1	0	0	0	2	0	12	6	1	332	94
	PA	96	100	100	100	87	98	47	78	98	59	**72**

Table 3. Accuracy assessment for the 30% threshold for west of the Continental Divide in Glacier National Park. Overall accuracy in bold.

		Visual Assessment										
Random Forest Prediction		Older Forest	Water	Snow/ Glacier	Shadow	Barren Rock	Burn	Shrub/ Deciduous	Young Forest	Dry Herb/ Grassland	Avalanche Track	UA
	Older Forest	99	0	0	0	0	0	1	7	0	30	72
	Water	0	88	0	0	0	0	0	0	0	0	100
	Snow/ Glacier	0	0	98	0	4	0	0	0	0	1	95
	Shadow	0	0	0	101	0	0	0	0	0	8	93
	Barren Rock	0	0	0	0	77	0	0	0	0	25	75
	Burn	0	0	0	0	4	88	0	0	5	88	48
	Shrub/ Deciduous	0	0	0	0	0	0	37	2	0	214	15
	Young Forest	5	0	0	0	0	0	2	60	0	1	88
	Dry Herb/ Grassland	0	0	0	0	0	1	4	0	45	12	73
	Avalanche Track	2	0	0	0	2	0	13	6	0	474	95
	PA	93	100	100	100	89	99	65	80	90	56	**73**

Table 4. Accuracy assessment for the 40% threshold for all of Glacier National Park. Overall accuracy in bold.

		Visual Assessment										
Random Forest Prediction		Older Forest	Water	Snow/ Glacier	Shadow	Barren Rock	Burn	Shrub/ Deciduous	Young Forest	Dry Herb/ Grassland	Avalanche Track	UA
	Older Forest	52	0	0	0	0	0	1	1	0	14	76
	Water	0	42	0	0	0	0	0	0	0	0	100
	Snow/ Glacier	0	0	51	0	3	0	0	0	0	1	93
	Shadow	0	0	0	61	0	0	0	0	0	1	98
	Barren Rock	0	0	0	0	44	0	0	0	0	3	94
	Burn	0	0	0	0	2	30	0	0	1	30	48
	Shrub/ Deciduous	0	0	0	0	0	0	21	0	0	66	24
	Young Forest	4	0	0	0	0	0	1	10	0	0	67
	Dry Herb/ Grassland	0	0	0	0	0	0	1	0	5	2	63
	Avalanche Track	1	0	0	0	0	0	3	0	0	169	98
	PA	91	100	100	100	90	100	78	91	83	59	**78**

Table 5. Accuracy assessment for the 40% threshold for east of the Continental Divide in Glacier National Park. Overall accuracy in bold.

		Visual Assessment										
Random Forest Prediction		Older Forest	Water	Snow/ Glacier	Shadow	Barren Rock	Burn	Shrub/ Deciduous	Young Forest	Dry Herb/ Grassland	Avalanche Track	UA
	Older Forest	47	0	0	0	0	0	0	6	0	16	68
	Water	0	46	0	0	0	0	0	0	0	0	100
	Snow/ Glacier	0	0	47	0	1	0	0	0	0	0	98
	Shadow	0	0	0	40	0	0	0	0	0	7	85
	Barren Rock	0	0	0	0	33	0	0	0	0	22	60
	Burn	0	0	0	0	2	58	0	0	4	58	48
	Shrub/ Deciduous	0	0	0	0	0	0	16	2	0	148	10
	Young Forest	1	0	0	0	0	0	1	50	0	1	94
	Dry Herb/ Grassland	0	0	0	0	0	1	3	0	40	10	74
	Avalanche Track	1	0	0	0	2	0	10	6	0	305	94
	PA	96	100	100	100	87	98	53	78	91	54	**69**

Table 6. Accuracy assessment for the 40% threshold for west of the Continental Divide in Glacier National Park. Overall accuracy in bold.

		Visual Assessment										
Random Forest Predication		Older Forest	Water	Snow/ Glacier	Shadow	Barren Rock	Burn	Shrub/ Deciduous	Young Forest	Dry Herb/ Grassland	Avalanche Track	UA
	Older Forest	99	0	0	0	0	0	1	7	0	30	72
	Water	0	88	0	0	0	0	0	0	0	0	100
	Snow/ Glacier	0	0	98	0	4	0	0	0	0	1	95
	Shadow	0	0	0	101	0	0	0	0	0	8	93
	Barren Rock	0	0	0	0	77	0	0	0	0	25	75
	Burn	0	0	0	0	4	88	0	0	5	88	48
	Shrub/ Deciduous	0	0	0	0	0	0	37	2	0	221	14
	Young Forest	5	0	0	0	0	0	2	60	0	1	88
	Dry Herb/ Grassland	0	0	0	0	0	1	4	0	45	12	73
	Avalanche Track	2	0	0	0	2	0	13	6	0	467	95
	PA	93	100	89	100	100	99	80	90	55	65	**72**

Table 7. Accuracy assessment for the 50% threshold for all of Glacier National Park. Overall accuracy in bold.

		Visual Assessment										
Random Forest Prediction		Older Forest	Water	Snow/ Glacier	Shadow	Barren Rock	Burn	Shrub/ Deciduous	Young Forest	Dry Herb/ Grassland	Avalanche Track	UA
	Older Forest	52	0	0	0	0	0	1	1	0	14	76
	Water	0	42	0	0	0	0	0	0	0	0	100
	Snow/ Glacier	0	0	51	0	3	0	0	0	0	1	75
	Shadow	0	0	0	61	0	0	0	0	0	1	98
	Barren Rock	0	0	0	0	44	0	0	0	0	3	94
	Burn	0	0	0	0	2	30	0	0	1	30	48
	Shrub/ Deciduous	0	0	0	0	0	0	21	0	0	70	23
	Young Forest	4	0	0	0	0	0	1	10	0	0	67
	Dry Herb/ Grassland	0	0	0	0	0	0	1	0	5	2	63
	Avalanche Track	1	0	0	0	0	0	3	0	0	165	98
	PA	91	100	100	100	90	100	78	91	83	58	**78**

Table 8. Accuracy assessment for the 50% threshold for east of the Continental Divide in Glacier National Park. Overall accuracy in bold.

		Visual Assessment										
Random Forest Prediction		Older Forest	Water	Snow/ Glacier	Shadow	Barren Rock	Burn	Shrub/ Deciduous	Young Forest	Dry Herb/ Grassland	Avalanche Track	UA
	Older Forest	47	0	0	0	0	0	0	6	0	16	68
	Water	0	0	0	0	46	0	0	0	0	0	100
	Snow/ Glacier	0	0	47	1	0	0	0	0	0	0	98
	Shadow	0	40	0	0	0	0	0	0	0	7	85
	Barren Rock	0	0	0	33	0	0	0	0	0	22	60
	Burn	0	0	0	2	0	58	0	0	4	58	48
	Shrub/ Deciduous	0	0	0	0	0	0	16	2	0	151	9
	Young Forest	1	0	0	0	0	0	1	50	0	1	94
	Dry Herb/ Grassland	0	0	0	0	0	1	3	0	40	10	74
	Avalanche Track	1	0	0	2	0	0	10	6	0	302	94
	PA	96	100	100	87	100	98	53	78	91	53	**69**

Table 9. Accuracy assessment for the 50% threshold for west of the Continental Divide in Glacier National Park. Overall accuracy in bold.

	Visual Assessment			
Random Forest Prediction		Non-Avalanche Track	Avalanche Track	UA
	Non-Avalanche Path	256,889	3,843	99
	Avalanche Path	40,837	5,638	88
	PA	86	60	**85**

Table 10. Accuracy assessment for the digitized set of avalanche tracks vs. the random forest model prediction at the 30% most likely class threshold. Classes were set in an avalanche track or not Boolean system for the accuracy assessment.